Power Converter Control Algorithm Design and Simulation for the NREL Next-Generation Drivetrain

July 8, 2013 — January 7, 2016

Douglas Blodgett, Michael Behnke, and William Erdman
DNV KEMA Renewables, Inc.
San Ramon, California

NREL Technical Monitor: Jonathan Keller

NREL is a national laboratory of the U.S. Department of Energy
Office of Energy Efficiency & Renewable Energy
Operated by the Alliance for Sustainable Energy, LLC

This report is available at no cost from the National Renewable Energy Laboratory (NREL) at www.nrel.gov/publications.

Subcontract Report
NREL/SR-5000-66486
August 2016

Contract No. DE-AC36-08GO28308

NREL
NATIONAL RENEWABLE ENERGY LABORATORY

Power Converter Control Algorithm Design and Simulation for the NREL Next-Generation Drivetrain

July 8, 2013 — January 7, 2016

Douglas Blodgett, Michael Behnke, and William Erdman
DNV KEMA Renewables, Inc.
San Ramon, California

NREL Technical Monitor: Jonathan Keller

Prepared under Subcontract No. NGB-3-23027

NREL is a national laboratory of the U.S. Department of Energy
Office of Energy Efficiency & Renewable Energy
Operated by the Alliance for Sustainable Energy, LLC

This report is available at no cost from the National Renewable Energy Laboratory (NREL) at www.nrel.gov/publications.

National Renewable Energy Laboratory
15013 Denver West Parkway
Golden, CO 80401
303-275-3000 • www.nrel.gov

Subcontract Report
NREL/SR-5000-66486
August 2016

Contract No. DE-AC36-08GO28308

This report is available at no cost from the National Renewable Energy Laboratory (NREL) at www.nrel.gov/publications.

Available electronically at SciTech Connect http:/www.osti.gov/scitech

Available for a processing fee to U.S. Department of Energy and its contractors, in paper, from:

U.S. Department of Energy
Office of Scientific and Technical Information
P.O. Box 62
Oak Ridge, TN 37831-0062
OSTI http://www.osti.gov
Phone: 865.576.8401
Fax: 865.576.5728
Email: reports@osti.gov

Available for sale to the public, in paper, from:

U.S. Department of Commerce
National Technical Information Service
5301 Shawnee Road
Alexandria, VA 22312
NTIS http://www.ntis.gov
Phone: 800.553.6847 or 703.605.6000
Fax: 703.605.6900
Email: orders@ntis.gov

Cover Photos by Dennis Schroeder: (left to right) NREL 26173, NREL 18302, NREL 19758, NREL 29642, NREL 19795.

NREL prints on paper that contains recycled content.

Table of Contents

1. Executive Summary 1-1
2. Introduction and Background 2-1
3. Grid Interconnection Requirements 3-1
   A. Purpose and Scope 3-1
   B. Eastern and Western Interconnections 3-2
   C. Electrical Reliability Council of Texas (ERCOT) Interconnection 3-4
   D. Hawaiian Electric Industries (HECO, MECO, HELCO) 3-5
   E. Puerto Rico Electric Power Authority (PREPA) 3-6
4. Converter and Generator Model 4-1
5. Asymmetrical Fault Response 5-1
   A. Introduction and Background 5-1
   B. Control Strategies and Simulation Results 5-3
      1. Instantaneous active-reactive control (IARC) 5-3
      2. Balanced positive-sequence control (BPSC) 5-4
      3. Positive- negative-sequence control (PNSC) 5-6
   C. Extraction of Line Voltage Waveform Symmetrical Components 5-8
   D. Line Synchronization 5-10
6. Symmetrical Fault Response 6-1
   A. Introduction and Background 6-1
   B. Power System and Control Model 6-1
   C. Simulations 6-1
   D. Observations 6-4
7. Frequency Response 7-1
   A. Introduction and Background 7-1
   B. Power System and Control Model 7-2
   C. Simulations 7-2
   D. Observations 7-4
8. Main Shaft Damping 8-1
   A. Introduction and Background 8-1
   B. Power System and Control Model 8-3
   C. Simulations 8-4
   D. Observations 8-6
9. Conclusions 9-1

Figures

Figure 3-1. Common elements of an interconnection requirements set 3-1
Figure 3-2. Geographic areas considered in interconnection requirements review 3-2
Figure 3-3. NERC PRC-024-01 voltage ride-through curve 3-4
Figure 3-4. NERC PRC-024-1 frequency ride-through curve 3-4
Figure 3-5. PREPA reactive power capability requirements for wind plants 3-7
Figure 3-6. PREPA voltage and frequency ride-through requirements for wind plants 3-8
Figure 4-1. Power circuit model 4-1
Figure 4-2. Current regulator and modulator model 4-2
Figure 5-1. IARC control model 5-3
Figure 5-2. Phase-to-Phase Fault at High Side of Step-up Transformer with IARC Method 5-4
Figure 5-3. BPSC control model 5-5
Figure 5-4. Phase-to-phase fault at high side of step-up transformer with BPSC method 5-6
Figure 5-5. PNSC control model 5-7
Figure 5-6. Phase-to-phase fault at high side of step-up transformer with PNSC method 5-8
Figure 5-7. Line voltage symmetrical components extraction with DSC method 5-9
Figure 5-8. Line voltage quadrature signal generation via SOGI and FLL 5-9
Figure 5-9. Line voltage symmetrical components extraction with SOGI quadrature signals 5-10
Figure 5-10. Open loop line synchronization model 5-10
Figure 5-11. Positive sequence PLL model 5-11
Figure 5-12. Negative sequence PLL model 5-11
Figure 6-1. Thirty-cycle fault to 90% terminal voltage (Reference: IEC 61400-12, Table 1, Case VD1) 6-2
Figure 6-2. Thirty-cycle fault to 50% terminal voltage (Reference: IEC 61400-12, Table 1, Case VD2) 6-3
Figure 6-3. Twelve-cycle fault to 20% terminal voltage (Reference: IEC 61400-12, Table 1, Case VD3) 6-3
Figure 6-4. Nine-cycle fault at high side of plant substation (Reference: FERC Order 661-A) 6-4
Figure 6-5. Nine-cycle fault at high side of local transformer, (Reference: Info, only) 6-4
Figure 7-1. Generator droop characteristic 7-1
Figure 7-2. Governor control model 7-2
Figure 7-3. Overfrequency transient at rated power 7-3
Figure 7-4. Underfrequency transient at rated power 7-3
Figure 7-5. Overfrequency transient at 50% power 7-4
Figure 7-6. Underfrequency transient at 50% power 7-4
Figure 8-1. Two-mass representation of torsional dynamics 8-1
Figure 8-2. Main shaft torsional model 8-3
Figure 8-3. Active main shaft damping control model 8-3
Figure 8-4. Power command step changes - no active damping 8-4
Figure 8-5. Power command step changes - with active damping 8-5
Figure 8-6. Nine-cycle symmetrical fault at high side of substation - no active damping 8-5
Figure 8-7. Nine-cycle symmetrical fault at high side of substation - with active damping 8-6

Tables

Table 4-1. Permanent Magnet Synchronous Generator Electrical Parameters 4-2
Table 5-1. Summary of Control Strategies with Unbalanced Line Voltages 5-8
Table 6-1. Symmetrical Fault Simulation Descriptions 6-2
Table 7-1. Frequency Response Simulation Descriptions 7-2
Table 8-1. Torsional Model Parameters (Referred to High Speed Shaft) 8-2
Table 8-2. Main Shaft Torsional Mode Simulations 8-4

1. Executive Summary

The National Renewable Energy Laboratory (NREL) and NREL Next-Generation Drivetrain Partners are developing a next-generation drivetrain (NGD) design as part of a Funding Opportunity Announcement award from the U.S. Department of Energy. The proposed NGD includes comprehensive innovations to the gearbox, generator, and power converter that increase the gearbox reliability and drivetrain capacity, while lowering deployment and operation and maintenance costs.

A key task within this development effort is the power converter fault control algorithm design and associated computer simulations using an integrated electromechanical model of the drivetrain. The results of this task will be used in generating the embedded control software to be utilized in the power converter during testing of the NGD in the National Wind Technology Center 2.5-MW dynamometer. A list of issues to be addressed with these algorithms was developed by review of the grid interconnection requirements of various North American transmission system operators, and those requirements that presented the greatest impact to the wind turbine drivetrain design were then selected for mitigation via power converter control algorithms. In summary, algorithms have been developed to address the following:

- *Asymmetrical Grid Fault Response*: The electrical topology selected for the drivetrain can result in power oscillations in the power converter and associated torque oscillations on the generator and gearbox during asymmetrical (line-to-line and line-to-ground) grid faults. These oscillations were quantified, and an algorithm was developed to mitigate them.

- *Symmetrical Grid Fault Response*: Power and torque transients associated with symmetrical (three-phase) grid faults were characterized under a variety of fault conditions to serve as an input to the gearbox design criteria.

- *Frequency Deviation Response*: An algorithm that allows the drivetrain to participate in Primary Frequency Response (modulation of output power in response to grid frequency deviations) was developed and simulated. This type of response is required by certain North American transmission system operators and is expected to see growing application as penetration of intermittent resources such as wind increases.

- *Main Shaft Torsional Mode Active Damping*: Symmetrical and asymmetrical faults are both intense sources of excitation for natural torsional resonances in the drivetrain that can result in damaging speed and torque oscillations. An algorithm that uses power converter DC link voltage sensing to provide active damping of the most significant of these torsional modes has been developed and demonstrated through computer simulation.

2. Introduction and Background

NREL and the NREL Next-Generation Drivetrain Partners developed a conceptual NGD design as part of a Funding Opportunity Announcement award from the U.S. Department of Energy. The proposed NGD includes comprehensive innovations to the gearbox, generator, and power converter that increase the gearbox reliability and drivetrain capacity while lowering deployment and operation and maintenance costs. The project was awarded continued funding to complete the design and build and then test the NGD in the National Wind Technology Center 2.5-MW dynamometer. The drivetrain design features:

- A high-reliability, low-cost, single-stage gearbox that incorporates hydrodynamic journal bearings, eliminates a significant portion of the bearings and gears used in a conventional gearbox, and incorporates additional planets and flex pins to increase capacity
- A variable-speed, permanent-magnet generator
- A three-level power converter that uses advanced materials for operation at higher voltages and incorporates fault control algorithms.

This document summarizes the results of the power converter fault control algorithm design and the computer simulation of these algorithms using an integrated electromechanical model of the drivetrain. These results will serve as the basis for the coding of the embedded control software to be utilized in the power converters during testing at the National Wind Technology Center.

The list of issues to be addressed with these algorithms was developed by review of the grid interconnection requirements of transmission system operators noted in Section 3. Those requirements that presented the greatest impact to the wind turbine drivetrain were then selected for further study. That list included the following:

- *Asymmetrical Fault Response*: With a passive rectifier between the generator and the DC link within the power converter, asymmetrical (line-to-line and line-to-ground) faults on the transmission network in the vicinity of the wind plant can result in power oscillations in the power converter and associated torque oscillations on the generator and gearbox. These oscillations were quantified and an algorithm developed to mitigate them. Results are described in Section 5.
- *Symmetrical Fault Response*: Power and torque transients associated with symmetrical (three-phase) faults on the neighboring transmission were characterized under a variety of fault conditions to serve as an input to the gearbox design criteria. Results are included in Section 6.
- *Frequency Deviation Response*: An algorithm that allows the drivetrain to participate in Primary Frequency Response (modulation of output power in response to grid frequency deviations) was developed and simulated. As described in Section 3, this type of response is already required in an island grid such as those in Hawaii and Puerto Rico as well as in the Electric Reliability Council of Texas (ERCOT) footprint. As wind penetration levels increase, it is expected that transmission system operators in the Eastern and Western Interconnections will impose similar requirements.

The algorithm and associated simulations addressing this requirement are described in Section 7.

- *Main Shaft Torsional Mode Active Damping*: The drivetrain has natural torsional modes that can be excited by a variety of stimuli (changes in wind speed, control actions, etc.). However, particularly intense sources of excitation for these resonances are symmetrical and asymmetrical grid faults that are electrically proximate to the wind plant. Excitation of these torsional modes in the drivetrain, through an almost instantaneous loss of load, can result in damaging speed and torque oscillations. An algorithm that uses power converter DC link voltage sensing to provide active damping of the most significant of these torsional modes has been developed and demonstrated through computer simulation. These results are described in Section 8.

For each interconnection requirement, simulations were performed using a common power circuit as well as common current regulation and pulse-width modulation schemes. These are described in Section 4. Each requirement described above was then addressed through algorithms that generate reference currents (or current commands) on the grid side of the power converter that address the particular requirement.

3. Grid Interconnection Requirements

A. Purpose and Scope

A set of wind turbine generator design criteria was established through a review of relevant North American grid interconnection requirements. Particular attention was given to requirements that impact the wind turbine generator drivetrain design, i.e., those that affect dimensioning of the gearbox, generator, or power converter.

In general, grid interconnection requirements are composed of a set of common elements that prescribe the response of the generation resource to deviations in grid voltage or frequency. The generator's response to particular events on the grid may be regulated through active power control, reactive power control, or disturbance ride-through as shown in Figure 3-1.

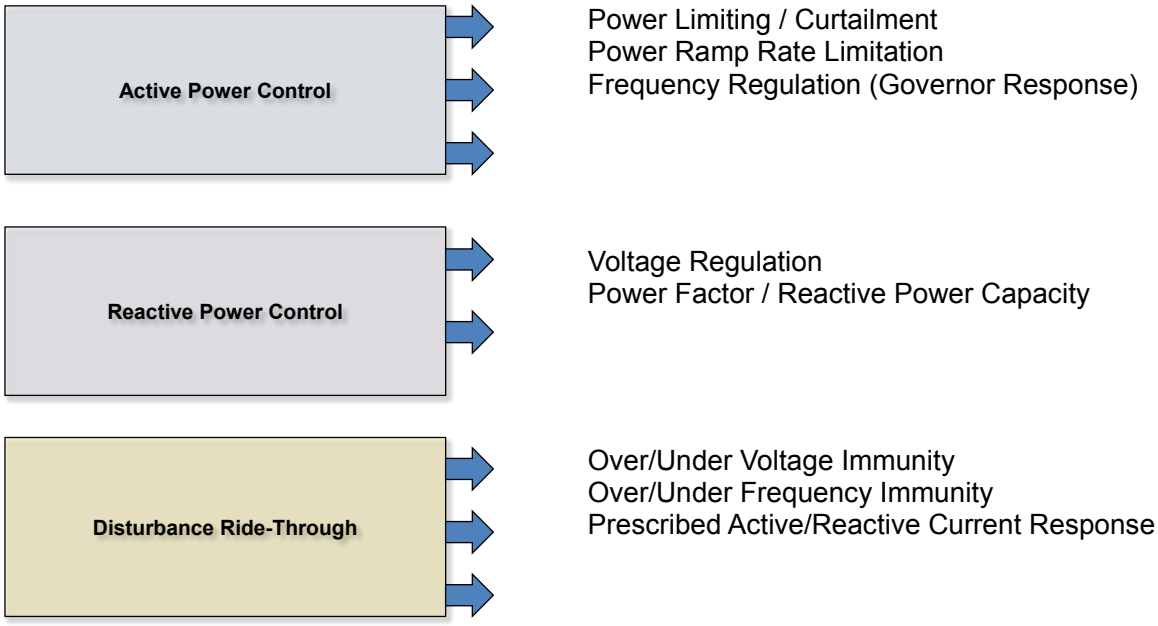

Figure 3-1. Common elements of an interconnection requirements set

The scope of the review was limited to U.S. geographic areas with a significant wind energy market potential. A further limitation of scope was to exclude single turbine or cluster interconnections at distribution voltage and to focus on transmission-interconnected wind plants, which comprise the vast majority of the wind turbine market in the United States. The following geographic areas shown in Figure 3-2 were considered in this review:

- Eastern and Western Interconnection: This area includes the entire continental United States outside of the ERCOT Interconnection.
- ERCOT Interconnection: The ERCOT footprint includes that portion of Texas not served from the Eastern or Western Interconnections.

- Hawaiian Electric Industries Utilities: This includes the three HEICO operating companies in the Hawaiian Islands – HECO, MECO, and HELCO.
- Puerto Rico Electric Power Authority: PREPA serves the entire island of Puerto Rico.

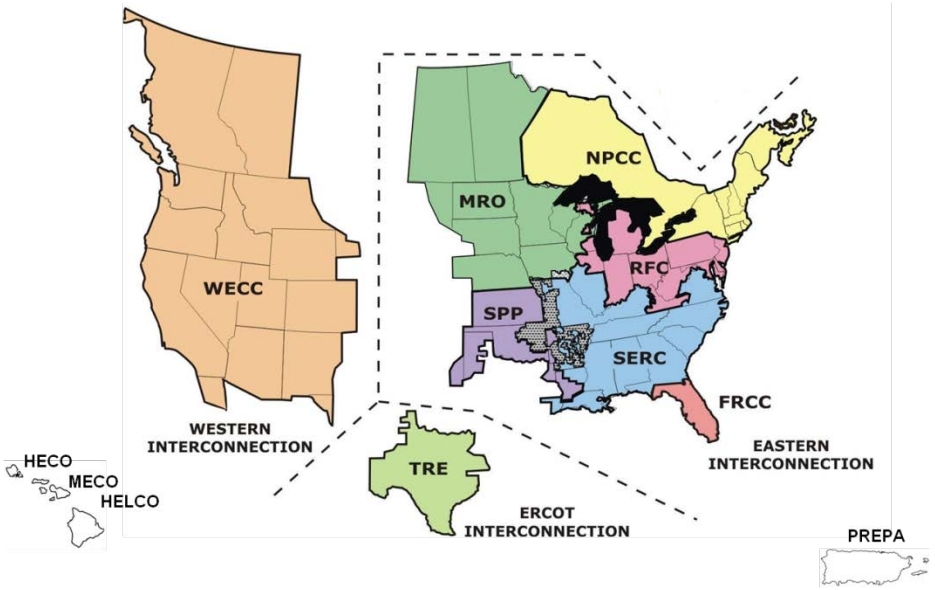

Figure 3-2. Geographic areas considered in interconnection requirements review[1]

B. Eastern and Western Interconnections

Transmission System Operators within the Eastern and Western Interconnections are regulated by the Federal Energy Regulatory Commission (FERC). The FERC has designated the North American Electric Reliability Corporation (NERC) as the Electric Reliability Organization responsible for reliability standards development and compliance enforcement in the United States. Generator owner/operators with interconnections to the Bulk Electric System (generally, facilities operating at ≥ 100 kV) and having individual unit capacity ≥ 20 MVA or aggregate plant capacity ≥ 75 MVA must comply with NERC Reliability Standards.[2] In addition, generator owner/operators must further operate their facilities in accordance with their Interconnection Agreements, the terms of which are largely dictated by FERC Orders.

The NERC standards with greatest impact to wind turbine generator drivetrain design considerations are:

- **VAR-002-2b**, *Generator Operation for Maintaining Network Voltage Schedules*. This is an active standard subject to enforcement.
- **PRC-024-1**, *Generator Frequency and Voltage Protective Relay Settings*. As of the date of this document, this standard has been filed with FERC and is pending regulatory approval.

The following FERC orders also impact wind turbine generator drivetrain design:

[1] Derived from NERC Interconnections Map, http://www.nerc.com/AboutNERC/keyplayers/Documents/NERC_Interconnections_Color_072512.jpg

[2] http://www.nerc.com/pa/Stand/Pages/AllReliabilityStandards.aspx?jurisdiction=United%20States

- **FERC Order 2003**, *Standard Interconnection Agreements and Procedures for Large Generators.*[3] This order is applicable to all generation facilities > 20 MW in rating.
- **FERC Order 2006**, *Standard Interconnection Agreements and Procedures for Small Generators.*[4] This order is applicable to generation facilities ≤ 20 MW.
- **FERC Order 661-A**, *Interconnection for Wind Energy.*[5] This order is applicable to wind generation facilities > 20 MW in rating.

With regard to active power control, at this time the NERC standards applicable to the Eastern and Western Interconnections place responsibility for frequency regulation and interchange control on the balancing authorities, not generator owners or generator operators, through the BAL family of NERC standards. Wind generation facilities are able, but not required, to offer active power-related ancillary services (e.g., frequency response, operating reserves) to the Balancing Authority. This could change as wind penetration levels increase.[6] Real-time curtailment capability is a growing requirement, however, as real-time markets (e.g., MISO, PJM, NYISO, CAISO, ERCOT) employ Security-Constrained Economic Dispatch systems.

Reactive power control is generally required in the Eastern and Western Interconnections. FERC Order 661-A requires that wind generation facilities > 20 MW in rating, where the Transmission Provider's System Impact Study shows a need to ensure safety or reliability, provide reactive power over a range of 0.95 leading to 0.95 lagging power factor at the point of interconnection. In addition, dynamic voltage support is required. NERC Standard VAR-002-2b requires generator operators to maintain a voltage or reactive power schedule as directed by the transmission operator.

Disturbance ride-through requirements in the Eastern and Western Interconnections are included in both FERC Order 661-A and NERC Standard PRC-024-1. FERC Order 661-A requires that wind generation facilities > 20 MW in rated remain on line during three-phase faults with normal clearing (up to nine cycles) and single line-to-ground faults with delayed clearing, for faults resulting in as low as zero voltage at the high side of the wind plant substation. NERC Standard PRC-024-1 requires that wind generation facilities ≥ 75 MVA in rating must set their protective relays such that generating units remain connected during voltage and frequency excursions at the point of interconnection defined by the curves in Figures 3-3 and 3-4, respectively.

[3] http://www.ferc.gov/industries/electric/indus-act/gi/stnd-gen.asp
[4] http://www.ferc.gov/industries/electric/indus-act/gi/small-gen.asp
[5] http://www.ferc.gov/industries/electric/indus-act/gi/wind.asp
[6] E. Ela et al., *Active Power Controls from Wind Power: Bridging the Gaps*, NREL/TP-5D00-60574, January 2014, http://www.nrel.gov/docs/fy14osti/60574.pdf

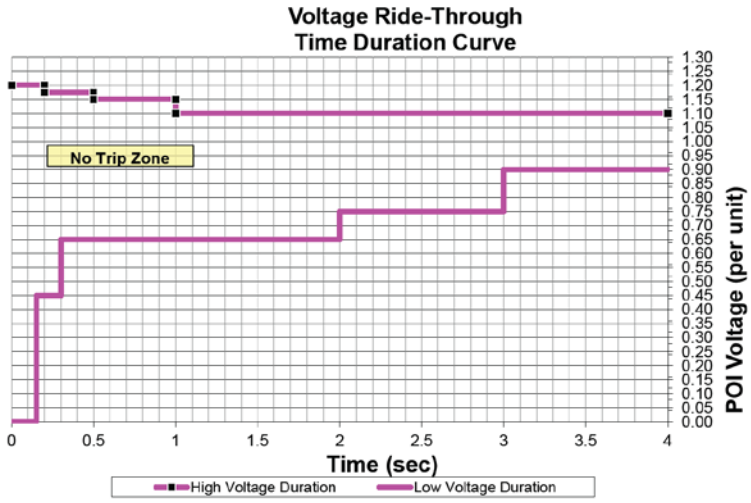

Figure 3-3. NERC PRC-024-01 voltage ride-through curve

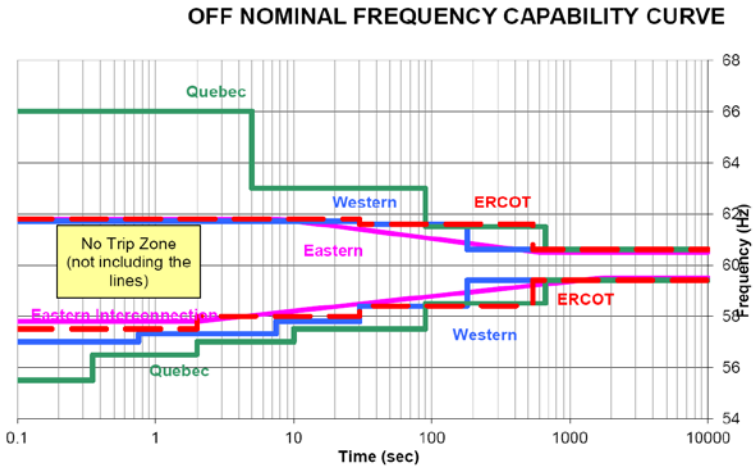

Figure 3-4. NERC PRC-024-1 frequency ride-through curve

C. Electrical Reliability Council of Texas (ERCOT) Interconnection

Transmission system operators within the ERCOT Interconnection are regulated primarily by the Texas Public Utility Commission. However, compliance with NERC standards (with regional variances) is still required for generator owner/operators with interconnections to the Bulk Electric System. In addition to NERC Standards VAR-002-2b and PRC-024-1 (discussed above with regard to the Eastern and Western Interconnection requirements), and addition NERC standard applies which is specific to the ERCOT Interconnection:

- **BAL-001-TRE-1**, *Primary Frequency Response in the ERCOT Region*. This standard became active and subject to enforcement beginning in April of 2014.

Generator owner/operators must further operate their facilities in accordance with the ERCOT Operating Guide (OG)[7] and Operating Protocols (OP).[8]

[7] http://www.ercot.com/mktrules/guides/noperating/cur

Unlike in the Eastern and Western Interconnections, NERC Standard BAL-001-TRE-1 requires that wind plants provide primary frequency response with a deadband ≤ ±0.017 Hz and a droop characteristic ≤ 5%. Further, wind plants are required to limit their ramp rates to 20% of nameplate MW per minute by ERCOT Operating Protocol 6.5.7.10.

Reactive power control capability is driven by ERCOT Operating Protocol 3.15. This OP requires that wind plants > 20 MVA provide voltage regulation over a reactive power range equivalent to 0.95 leading to 0.95 lagging power factor at nameplate MW for any active power level ≥ 10% of nameplate.

Finally, disturbance ride-through requirements are specified in ERCOT Operating Guidelines 2.9.1 and 2.6.2 for voltage and frequency deviations, respectively. OG 2.9.1 and OG 2.6.2 each refer to the ride-through curves from NERC Standard PRC-024-01 shown in Figures 3-3 and 3-4, above.

D. Hawaiian Electric Industries (HECO, MECO, HELCO)

Hawaiian Electric Industries is the parent company to operating companies Hawaiian Electric (HECO), Maui Electric (MECO) and Hawaii Electric Light (HELCO), which serve the islands of Oahu, Maui, and Hawaii, respectively. These companies are regulated by the Hawaii Public Utility Commission. NERC standards and FERC orders are not applicable.

Interconnection requirements for wholesale generation are negotiated on a project-by-project basis through power purchase agreement appendices.[9] Specific interconnection provisions result from an Interconnection Requirements Study and application of internal Hawaiian Electric Industries planning standards, which are not publicly available at this time.

Typical requirements from an Interconnection Requirements Study that necessitate active power control include:

- Provision of primary frequency response with no deadband and a 5% droop characteristic
- Limitation of instantaneous ramp rates to 1 MW/2-second scan and average ramp rates to 0.3 MW/2-second scan for any 60-second period
- Response to curtailment control interfaces immediately and with minimum rate response of 5% of nameplate MW per minute.

Reactive power requirements typically include:

- Control of reactive power by automatic voltage regulation to 0.5% of a scheduled voltage
- Reactive power capability from 0.90 leading to 0.85 lagging power factor at the point of interconnection.

---

[8] http://www.ercot.com/mktrules/nprotocols/current

[9] Examples include:

- https://www.hawaiianelectric.com/Documents/clean_energy_hawaii/producing_clean_energy/waivered_projects/attachment_1.pdf
- https://www.hawaiianelectric.com/Documents/clean_energy_hawaii/producing_clean_energy/waivered_projects/2013_february_model_renewable_as_available_energy.pdf

Typical disturbance ride-through requirements reflect the island nature of the power system:

- Low voltage ride-through down to zero volts on any phase at the point of interconnection for up to 600 ms, with active power recovery to 90% of pre-fault level within 1 second
- High voltage ride-through requirements of up to 120% on any phase for 1 second
- Continuous operation between 57.5 Hz and 61.5 Hz grid frequency.

E. Puerto Rico Electric Power Authority

Until August 2014, Puerto Rico Electric Power Authority (PREPA), as an agency of the Puerto Rican government, was self-regulated. The newly created Energy Regulatory Commission has not yet addressed issues related to reliability standards. As in Hawaii, NERC standards and FERC orders do not apply. Interconnection requirements for wholesale generation take the form of Minimum Technical Requirements documents recently established by PREPA for renewable resources.[10]

The Minimum Technical Requirements for wind plants require active power control and/or energy storage to meet the following requirements:

- Primary frequency response with a 5% droop characteristic up to ±10% of nameplate MW, with a step response of one second or less
- Inertial response capability (but with undefined requirements)
- Limitation of ramp rates to ±10% of nameplate MW per minute.

Further Minimum Technical Requirements require reactive power control capability, including:

- Provision of voltage regulation capability with < 1 second step response
- Reactive power range equivalent to 0.85 leading to 0.85 lagging power factor at nameplate MW for any active power level. A portion of this must be dynamic per Figure 3-5.

[10] http://www.nrel.gov/docs/fy14osti/57089.pdf

Reactive Power Capability Requirements

- Applies at POI
- Dynamic capability must be capable of 1-second step response
- Steady-state capability may include switched capacitors/reactors

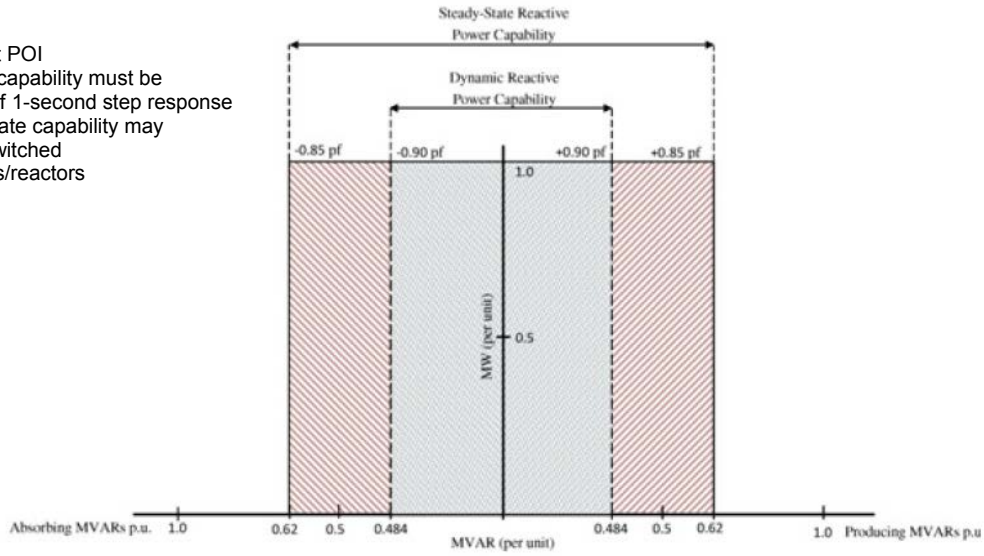

Figure 3-5. PREPA reactive power capability requirements for wind plants

Additional Minimum Technical Requirements address disturbance ride-through requirements. Wind plants are required to ride through the voltage and frequency disturbances defined in Figure 3-6. In addition, for disturbances that result in point of interconnection voltage dips below 85% of nominal, reactive current injection in an amount proportional to the magnitude of the voltage dip is required.

Ride-Through Requirements

Voltage Ride-Through

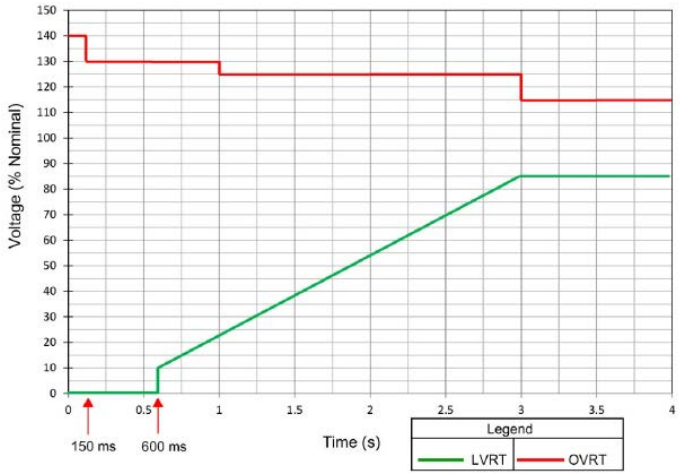

Frequency Ride-Through

• 57.5 - 61.5 Hz	No tripping (continuous)
• 61.5 - 62.5 Hz	30 sec
• 56.5 - 57.5 Hz	10 sec
• < 56.5 or > 62.5 Hz	Instantaneous trip

- Apply at POI
- Symmetrical or asymmetrical disturbances
- Programmed reactive current injection for voltages below 0.85 pu

Figure 3-6. PREPA voltage and frequency ride-through requirements for wind plants

4. Converter and Generator Model

The integrated electromechanical and electromagnetic power circuit model of the drivetrain, implemented in the *PSIM*® simulation environment,[11] is shown in Figure 4-1. The model is a representation of one of four stator winding quadrants of the permanent magnet synchronous generator. Each quadrant has a nominal 375 kW rating, and the four quadrants are operated in parallel with identical currents between them. Thus, the simulated power and torque values can be extended to the full 1.5 MW rating of the drivetrain by multiplying the results by a factor of four.

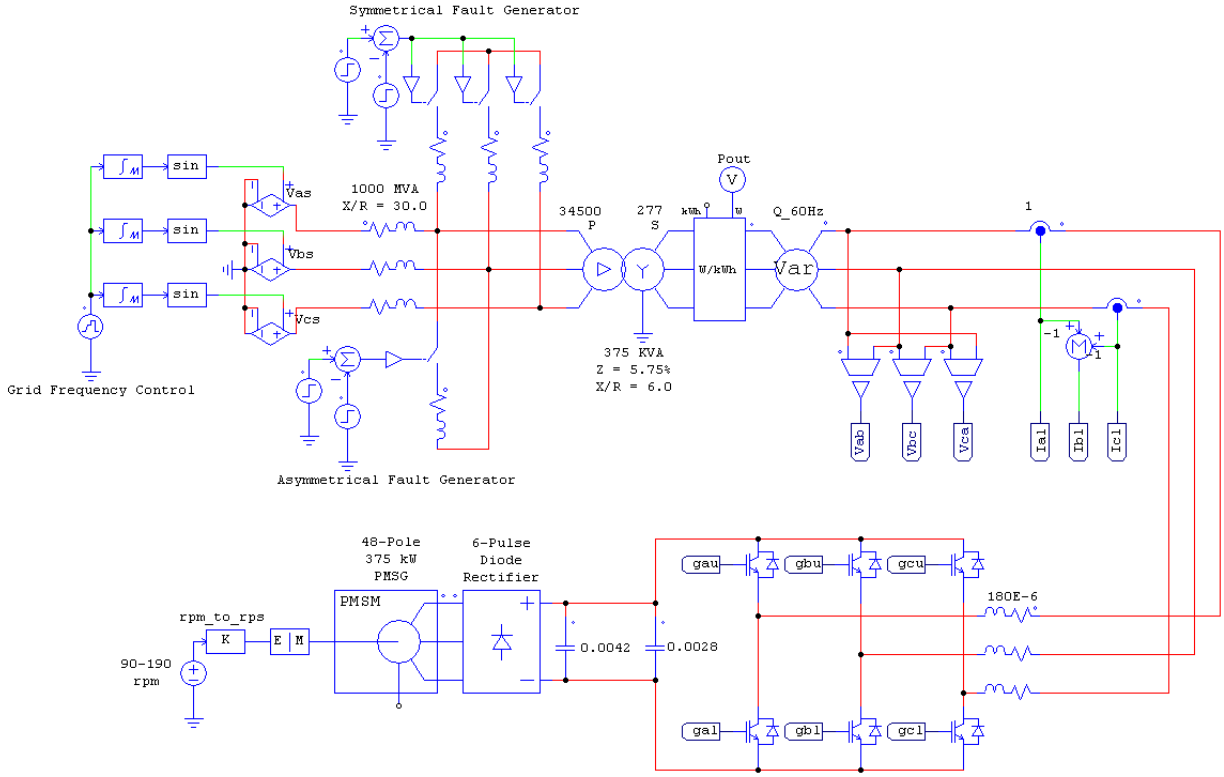

Figure 4-1. Power circuit model

The grid is represented by a balanced three-phase set of voltage sources behind a resistance-inductance source impedance. The magnitude of the voltage sources are fixed at 19.9 kV_{LN} (or 34.5 kV_{LL}), with frequency set by the magnitude of the DC voltage source labeled "Grid Frequency Control." The source impedance is 1,000 MVA with an X/R ratio of 30, which is within the typical range for a 34.5 kV collection system in a 100 MW wind plant. Symmetrical (three-phase) and asymmetrical (phase-to-phase) faults are simulated by switching shunt impedances that form a voltage divider with the source impedance.

The converter is interfaced with the collection system via a 34.5 kV to 480 V delta-wye connected transformer. The converter active (*Pout*) and reactive (*Q_60Hz*) power outputs are monitored at the low

[11] http://powersimtech.com/products/psim/

voltage winding of this transformer. Terminal voltage (*Vab*, *Vbc*, *Vca*) and current (*Ial*, *Ibl*, *Icl*) feedback signals are provided to the power converter controller.

The power converter is of the voltage source type. Its input capacitance and output inductance are dimensioned, in units of F and H, respectively, as shown in Figure 4-1. Insulated gate bipolar transistor gating signals from the power converter controller are labeled *gxy*, where *x* is the pole (a, b or c phase) and *y* is the upper (u) or lower (l) device in that pole.

The power converter's DC link is fed from the rectified output of a permanent magnet synchronous generator with parameters shown in Table 4-1.

Table 4-1. Permanent Magnet Synchronous Generator Electrical Parameters

Parameter	Value
R_s, Stator Resistance	0.0144 Ω
L_d, D-axis Inductance	1.4 mH
L_q, Q-axis Inductance	1.4 mH
k_v, Voltage Constant	7.4 $V_{peak,LL}$/rpm
P, # of Poles	48
J, Moment of Inertia	1,350 kg-m^2
B_m, Damping Coefficient	0 N-m-s

The wind turbine is represented by the constant-speed (controllable over a range from 90 to 190 rpm), single-mass mechanical model shown in Figure 4-1 for the fault and frequency response simulations. It was replaced with a two-mass torsional model for simulation of the main shaft resonant mode damping. Details on the two-mass torsional model are included in Section 8.

The current regulation and modulation model utilized for all simulations is shown in Figure 4-2, with the insulated gate bipolar transistor gating and current feedback signals defined in Figure 4-1. A sine-triangle pulse-width modulation (PWM) scheme with a 4 kHz carrier frequency is used. By using a common power circuit, current regulator, and pulse-width modulator, each grid interconnection requirement can be addressed through algorithms that generate reference currents (*Ia_ref*, *Ib_ref,* and *Ic_ref*) that address that particular requirement. Details regarding the generation of those reference currents are described in subsequent sections of this document.

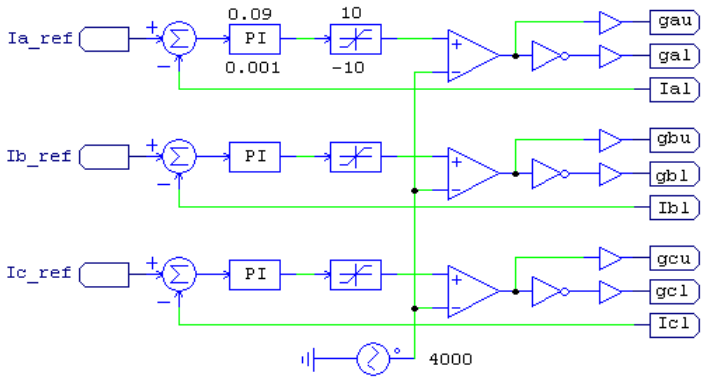

Figure 4-2. Current regulator and modulator model

5. Asymmetrical Fault Response

A. Introduction and Background

In generating current references for use in grid interactive current-regulated PWM inverters, ideally three performance objectives will be met:

1. The current references will result in a constant active power output, so as to minimize oscillations of the DC link voltage.
2. The current references will result in a constant reactive power output, so as to minimize oscillations of the AC line voltage.
3. The current references will be sinusoidal, so as to minimize harmonics in the output current waveform.

In practice, all three of these objectives can be achieved if the AC line voltages are balanced (i.e., consist of pure positive sequence voltage). However, if the line voltages are unbalanced, some compromises must be made in one or more of these performance criteria.

First, consider a control strategy that maintains sinusoidal current references. In a three-phase, three-wire system, the sinusoidal unbalanced line voltages or currents can be resolved into two sets of balanced voltages or current with opposite phase rotation: 1) the positive sequence (i.e., *a-b-c*) set, and 2) the negative sequence set (*a-c-b*).[12,13] The voltage and current vectors are, therefore:

$$\bar{v} = \begin{bmatrix} v_a \\ v_b \\ v_c \end{bmatrix} = \bar{v}^p + \bar{v}^n = \begin{bmatrix} v_a^p \\ v_b^p \\ v_c^p \end{bmatrix} + \begin{bmatrix} v_a^n \\ v_b^n \\ v_c^n \end{bmatrix} \qquad (5\text{-}1)$$

$$\bar{\imath} = \begin{bmatrix} i_a \\ i_b \\ i_c \end{bmatrix} = \bar{\imath}^p + \bar{\imath}^n = \begin{bmatrix} i_a^p \\ i_b^p \\ i_c^p \end{bmatrix} + \begin{bmatrix} i_a^n \\ i_b^n \\ i_c^n \end{bmatrix} \qquad (5\text{-}2)$$

In the presence of unbalanced line voltages and/or output currents, the time-domain active power and reactive power outputs each consist of two terms. The first is a constant (DC) term. The second is an oscillating term with a frequency of twice the fundamental line frequency. The DC terms result from the interaction of the symmetrical voltage and current vectors in the same phase sequence, while the oscillating terms result from cross coupling of the symmetrical voltages and currents with different phase sequence as follows[14]:

---

[12] C.L. Fortescue, "Method of Symmetrical Co-ordinates Applied to the Solution of Polyphase Networks," *A.I.E.E. Trans.*, vol. 37, June 1918, pp. 1027-1140.

[13] W.V. Lyon, *Application of the Method of Symmetrical Components*, New York: McGraw-Hill, 1937.

[14] H. Akagi, Y. Kanazawa, and A. Nabae, "Instantaneous Reactive Power Compensator Comprising Switching Devices Without Energy Storage Components," *IEEE Trans. Ind. Appl.*, vol. IA-20, no. 3, 1984, pp. 625-630.

$$p = \bar{v} \cdot \bar{\imath} = \underbrace{\bar{v}^p \cdot \bar{\imath}^p + \bar{v}^n \cdot \bar{\imath}^n}_{P_{dc}} + \underbrace{\bar{v}^p \cdot \bar{\imath}^n + \bar{v}^n \cdot \bar{\imath}^p}_{P_{osc}} \quad (5\text{-}3)$$

$$q = |\bar{v} \times \bar{\imath}| = \underbrace{|\bar{v}^p \times \bar{\imath}^p| + |\bar{v}^n \times \bar{\imath}^n|}_{Q_{dc}} + \underbrace{|\bar{v}^p \times \bar{\imath}^n| + |\bar{v}^n \times \bar{\imath}^p|}_{Q_{osc}} \quad (5\text{-}4)$$

Note that in (5-3) and (5-4) there are potentially four terms (two DC, two oscillating) that can be controlled, but only two vectors ($\bar{\imath}^p$ *and* $\bar{\imath}^n$) by which to control them. This means that two terms can be actively controlled, with the remaining two terms a consequence of those control choices. For example, suppose it is desired to control the constant active power term to some value P_{dc} and to cancel the oscillating active power term (i.e., set P_{osc} to zero) to minimize oscillations of the DC link voltage. From (5-3), this implies the following:

$$P_{dc} = \bar{v}^p \cdot \bar{\imath}^p + \bar{v}^n \cdot \bar{\imath}^n \quad (5\text{-}5)$$

$$0 = \bar{v}^p \cdot \bar{\imath}^n + \bar{v}^n \cdot \bar{\imath}^p \quad (5\text{-}6)$$

From (5-6), the desired negative sequence current is:

$$\bar{\imath}^n = -\frac{\bar{v}^p \cdot \bar{\imath}^p}{\|\bar{v}^p\|^2} \bar{v}^n \quad (5\text{-}7)$$

The desired positive sequence current can be derived from (5-5) and (5-7) as:

$$\bar{\imath}^p = \frac{P_{dc}}{\|\bar{v}^p\|^2 - \|\bar{v}^n\|^2} \bar{v}^p \quad (5\text{-}8)$$

Note that the negative and positive sequence current vectors in (5-7) and (5-8) are in phase with the negative and positive sequence voltage vectors, respectively. This means that the cross products represented by the first two terms in (5-4) are zero; therefore, Q_{dc} is zero. The third and fourth terms in (5-4) that compose Q_{osc}, however, are nonzero. Performance objectives #1 and #3 have been achieved at the sacrifice of #2.

Next, consider a strategy that allows for nonsinusoidal current references. One such control strategy is Instantaneous Active-Reactive Control (IARC)[15], which drives active and reactive components of current based on inverter output conductance and susceptance. The desired current vector is:

$$\bar{\imath} = \bar{\imath}_{active} + \bar{\imath}_{reactive} = \frac{P_{dc}}{\|\bar{v}\|^2} \bar{v} + \frac{Q_{dc}}{\|\bar{v}\|^2} \bar{v}_{\perp} \quad (5\text{-}9)$$

where $\bar{v}_{\perp}$ is a +90° phase shifted version of the voltage vector $\bar{v}$. This strategy allows for control of nonzero DC components of active and reactive power without oscillations of either. However, since $\|\bar{v}\|$ becomes oscillatory under unbalanced line voltage conditions, the current references become distorted. In addition to creating challenges in the design of the current regulator, these distorted references result in distorted output currents, creating the potential for voltage distortion and noncompliance with harmonic current limitations imposed by industry standards such as IEEE 519

[15] P. Rodriguez, A.V. Timbus, R. Teodorescu, M. Liserre, and F. Blaabjerg, "Independent PQ Control for Distributed Power Generation Systems under Grid Faults," *IECON 2006 - 32nd Annual Conference of IEEE Industrial Electronics,* pp. 5185-5190, 6-10 Nov. 2006.

even under “normal” (unfaulted) levels of voltage imbalance. Performance objectives #1 and #2 have been achieved at the sacrifice of #3.

B. Control Strategies and Simulation Results

As shown above, the selection of a control strategy from which to derive the current references has to be made by trading off performance metrics. In addition to the two strategies previously described, and third one is considered here. All three are based on the work by Rodriguez et al.[16] and have been implemented as *PSIM*® models.

1. Instantaneous active-reactive control

As described above, the instantaneous current reference vector is generated via Eq. 5-9. This control method has been implemented in *PSIM*® in the two-phase stationary reference frame, shown in Figure 5-1. *Valpha* and *Vbeta* are the line voltages provided by the line synchronization scheme (see Section 5.D below) and *Ia_ref, Ib_ref* and *Ic_ref* are the resulting current references in the natural reference frame.

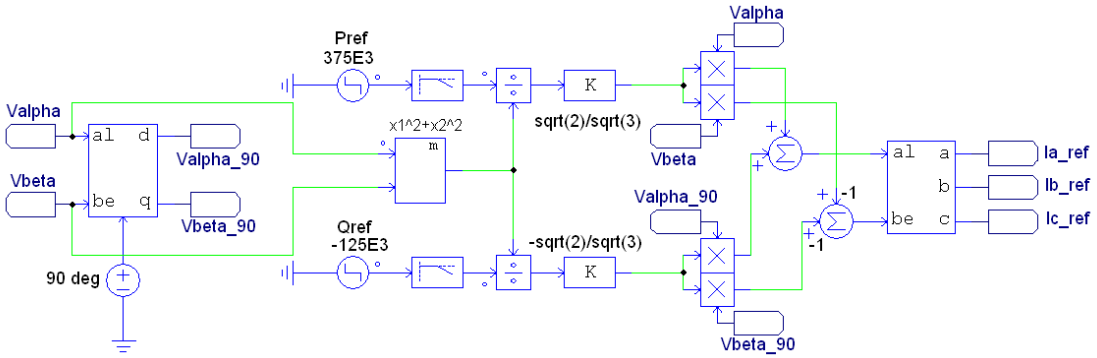

Figure 5-1. Instantaneous active-reactive control model

No knowledge of the symmetrical components of the line voltages is necessary, and the method allows, in theory, for control of constant, oscillation-free active and reactive power control. However, the current references are highly nonsinusoidal when the line voltages are unbalanced, as shown in the simulation results of Figure 5-2 for a bolted phase-to-phase fault at the high side of the wind turbine generator step-up transformer. In this simulation, the converter model has been replaced by a three-phase set of ideal current amplifiers. Plots in Figure 5-2 includes line converter line voltages (top pane), reference currents (center pane), and active and reactive power (bottom pane).

[16] P. Rodriguez, A.V. Timbus, R. Teodorescu, M. Liserre, and F. Blaabjerg, "Independent PQ Control for Distributed Power Generation Systems under Grid Faults," *IECON 2006 - 32nd Annual Conference of IEEE Industrial Electronics*, pp. 5185-5190, 6-10 Nov. 2006.

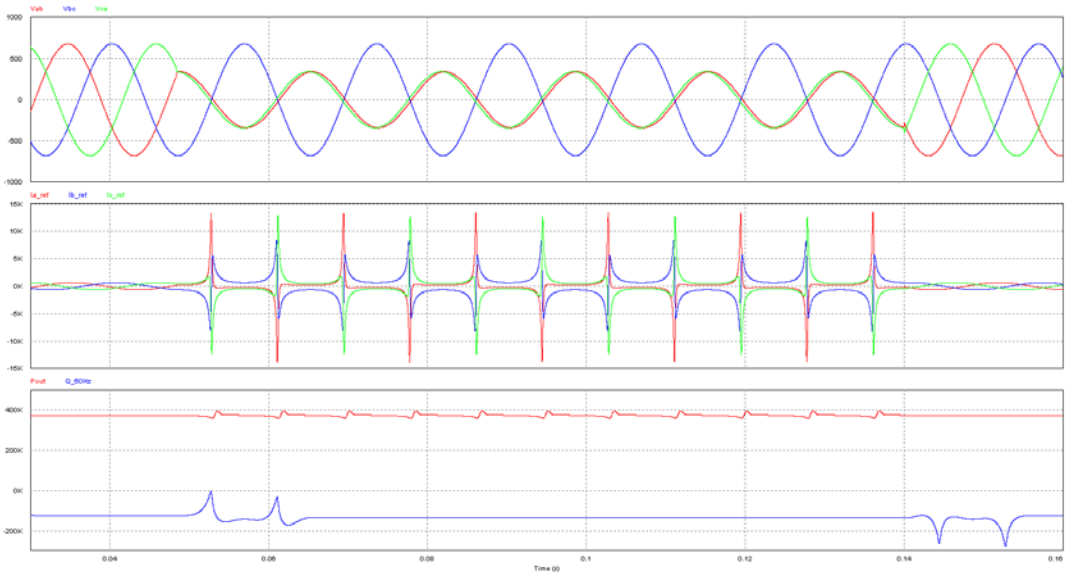

Figure 5-2. Phase-to-phase fault at high side of step-up transformer with instantaneous active-reactive control method

Figure 5-2 demonstrates that the instantaneous active-reactive control (IARC) method requires very high peak current capability and control bandwidth. In addition, it is highly sensitive to source impedance. Despite the theoretical capability to provide instantaneous control of active and reactive power (i.e., eliminate oscillations in both), it is impractical to implement not only on the NREL NGD, but likely on any commercial wind turbine.

2. Balanced positive-sequence control

With this control method, the inverter is controlled to generated positive sequence sinusoidal current references, only. Setting $\vec{\imath}^{n}$ to zero in Eq. (5-3) and (5-4) results in the following positive sequence current vector:

$$\vec{\imath}^{p} = \vec{\imath}^{p}_{active} + \vec{\imath}^{p}_{reactive} = \frac{P_{dc}}{\|\vec{v}^{p}\|^{2}}\vec{v}^{p} + \frac{Q_{dc}}{\|\vec{v}^{p}\|^{2}}\vec{v}^{p}_{\perp} \qquad (5\text{-}10)$$

A *PSIM*® model of this control method in the synchronous (dq) reference frame is shown in Figure 5-3. Current limits have been selected to allow for the reference active and reactive power outputs at 90% of nominal line voltage, and are implemented by logic in the “Dynamic Conductance Limiter” and “Dynamic Susceptance Limiter” blocks.

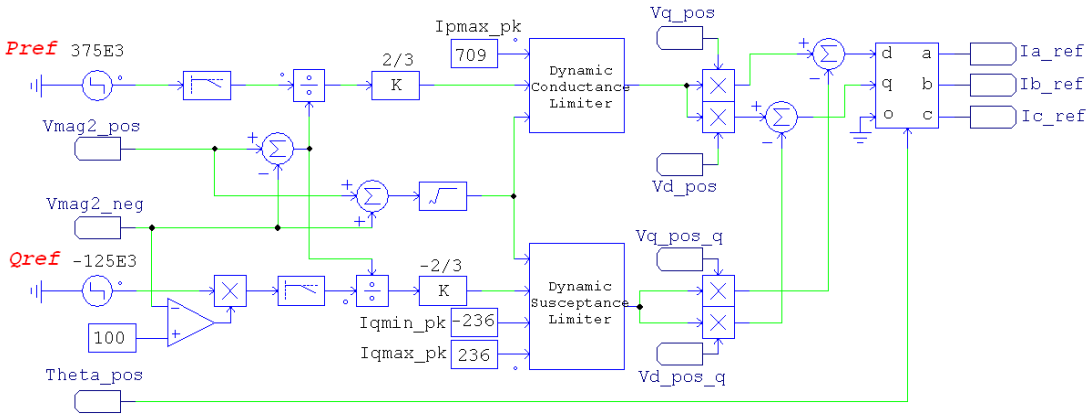

Figure 5-3. Balanced positive-sequence control model

Note that this method requires that the positive sequence voltage vector $\bar{v}^p$ (*Valpha_pos* and *Vbeta_pos*) be extracted from the line voltages (see Section 5.C). The current references are both balanced and sinusoidal. However, oscillations of both active and reactive power will occur with unbalanced voltages due to the interaction of the positive sequence current vector with the negative sequence voltage vector. With the electrical topology of the NREL NGD, the active power oscillations result in DC bus voltage oscillations which, in turn, subject the generator and gearbox to oscillating torques at twice the grid frequency during these faults. This can be seen in the simulation results of Figure 5-4 for a bolted phase-to-phase fault at the high side of the wind turbine generator step-up transformer. Note that the reactive power channel is the 60 Hz component only, not instantaneous reactive power, which is why the reactive power oscillations are not visible. In this simulation, the full electromagnetic and electromechanical drivetrain model of Figure 4-1 has been utilized, and the line currents have been synchronized to the line voltages using the positive sequence phase locked loop (PLL) shown in Figure 5-11. Generator electromagnetic torque is shown in the lower pane.

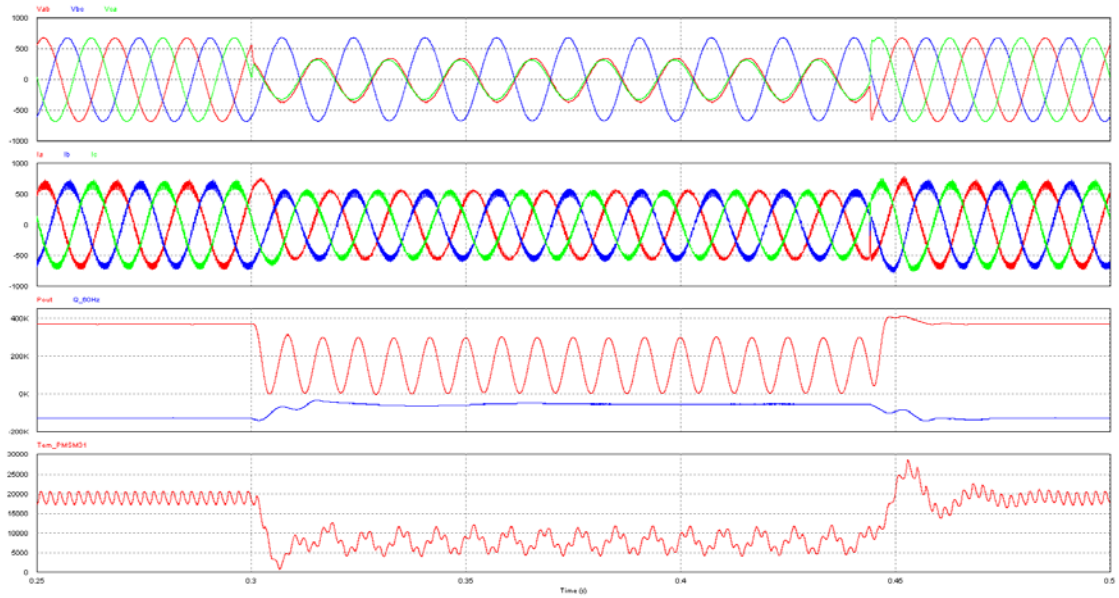

Figure 5-4. Phase-to-phase fault at high side of step-up transformer with balanced positive-sequence control method

This method can be implemented on the NREL NGD so long as the 120 Hz torque oscillations seen in Figure 5-4 during the fault are determined to be within the gearbox design criteria.

3. Positive-negative-sequence control

This method allows for control of two of the following four terms from Eq. (5-3) and (5-4): P_{dc}, Q_{dc}, P_{osc}, and Q_{osc}, and provides for sinusoidal, though unbalanced, current references with unbalanced line voltages. Controlling P_{dc} and Q_{dc} can be done via balanced positive-sequence control (BPSC), and control of Q_{osc} necessarily results in zero average active power, undesirable in this application. So this method is best suited to controlling P_{dc} and P_{osc} via Eq. (5-7) and (5-8) so long as controlled reactive current injection during unbalanced faults is not a requirement.

Implementation of these equations in *PSIM*® in the synchronous (dq) reference frame is shown in Figure 5-5. Note that a switch is used to drive Q_{dc} to zero when the magnitude of the negative sequence voltage vector exceeds some threshold (10 V, in this case) so that P_{osc} can be held to zero during these conditions.

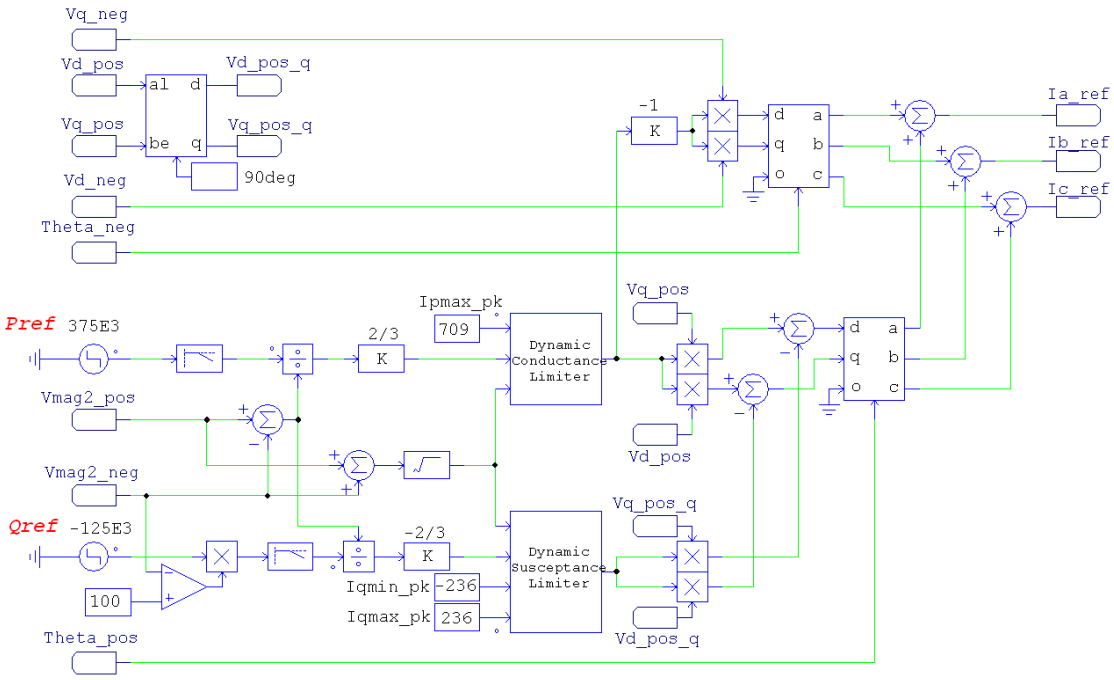

Figure 5-5. PNSC control model

This method requires that both the positive and negative sequence voltage vectors $\bar{v}^p$ (*Valpha_pos* and *Vbeta_pos*) and $\bar{v}^n$ (*Valpha_neg* and *Vbeta_neg*) be extracted from the line voltages (see Section 5.C below). While active power oscillations can be eliminated with this method, reactive power oscillations will occur with unbalanced voltages due to cross coupling of the positive and negative sequence networks. This can be seen in the simulation results of Figure 5-6 for a bolted phase-to-phase fault at the high side of the wind turbine generator step-up transformer. As in the previous simulation, the full electromagnetic and electromechanical drivetrain model of Figure 4-1 has been utilized, and the line currents have been synchronized to the line voltages using the positive sequence and negative sequence PLLs shown in Figure 5-11 and Figure 5-12, respectively.

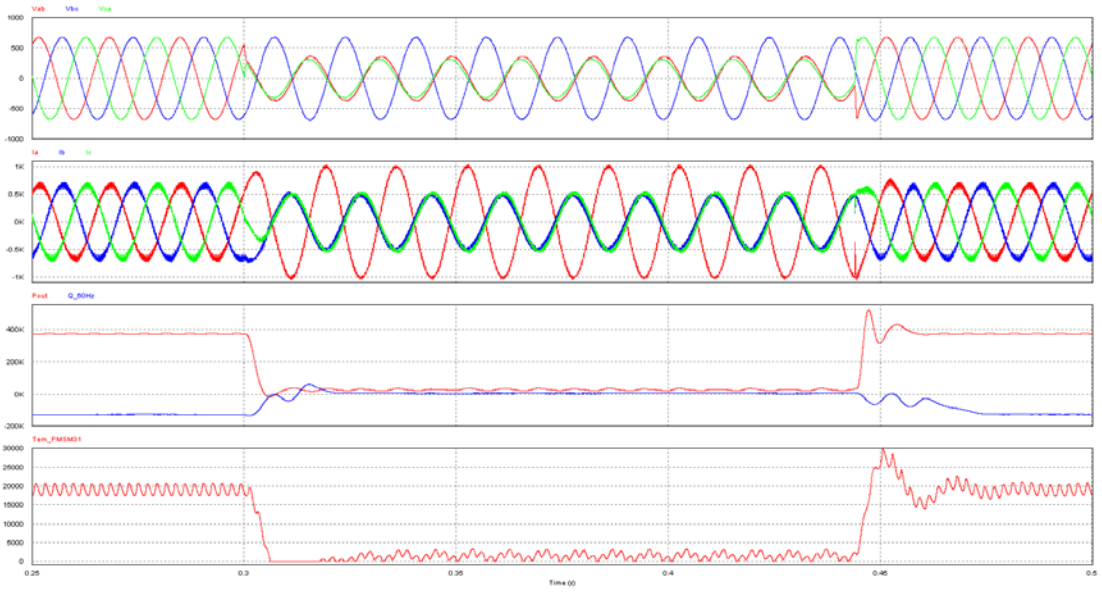

Figure 5-6. Phase-to-phase fault at high side of step-up transformer with positive-negative-sequence control method

This method can be implemented on the NREL NGD if it is determine that the 120 Hz torque oscillations seen in Figure 5-6 during the fault are determined to be outside of the gearbox design criteria. However, as can be seen in the simulation results, the power converter must be capable of providing short-term current of approximately 156% of its continuous rating.

Table 5-1 summarizes the requirements and benefits of the three control methods investigated.

Table 5-1. Summary of Control Strategies with Unbalanced Line Voltages

Method	Sinusoidal Currents	Balanced Currents	Power Oscillation Cancellation	Symmetrical Component Extraction
IARC	No	No	Yes	No
BPSC	Yes	Yes	No	Yes
PNSC	Yes	No	Yes	Yes

C. Extraction of Line Voltage Waveform Symmetrical Components

As noted above, an algorithm to extract the instantaneous symmetrical components from the unbalanced line voltages is necessary to implement the BPSC and positive-negative-sequence control (PNSC) strategies. Numerous methods for doing so are described in the literature.[17] Regardless of the method chosen, it is necessary to construct quadrature (90-degree delayed) line voltage signals. A simple method of constructing these quadrature signals is Delayed Signal Cancellation (DSC), shown in Figure 5-7. This method is a reformulation of Fortescue's equations

[17] G. Saccomando and J. Svensson, "Transient operation of grid-connected voltage source converter under unbalanced voltage conditions," *Thirty-Sixth IAS Annual Meeting. Conference Record of the 2001 IEEE Industry Applications Conference, 2001*, vol. 4, pp. 2419-2424, Sept. 30–Oct. 4, 2001.

using a 90-degree lag operator as opposed to the 120-degree operator used when the equations are expressed in the phasor domain. The two-phase stationary frame voltages *Valpha* and V*beta* are buffered for ¼ of one line cycle to produce the quadrature voltage signals.

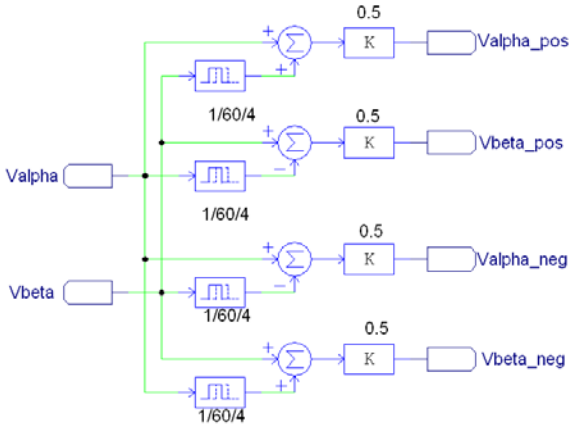

Figure 5-7. Line voltage symmetrical components extraction with DSC method

The disadvantage to this method is the errors that are introduced when operating at off-nominal grid frequency. The delay time corresponding to ¼ of a line cycle varies with frequency, of course. An improvement to the DSC scheme is the second order generalized integrator (SOGI) with frequency locked loop (FLL).[18] This method is frequency adaptive, but requires an estimate of line frequency as an input. For this reason, it is better suited for use with closed-loop (e.g., PLL) line synchronization schemes (see Section 5.D below) that inherently provide this frequency estimate. A *PSIM*® model that implements this scheme is shown in Figure 5-8 and Figure 5-9. The *filter_comp* signal compensates for the phase lag in the low-pass filters. The *freq_est* signal is an estimate of line frequency coming from another source (e.g., a PLL).

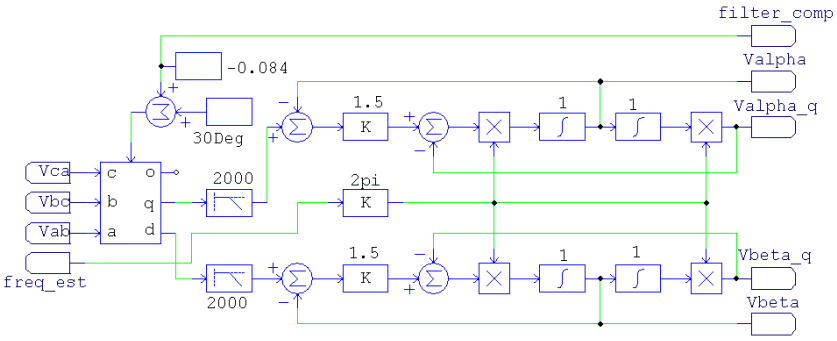

Figure 5-8. Line voltage quadrature signal generation via SOGI and FLL

[18] P. Rodriguez, A. V. Timbus, R. Teodorescu, M. Liserre, and F. Blaabjerg, "Flexible Active Power Control of Distributed Power Generation Systems During Grid Faults," *IEEE Transactions on Industrial Electronics,* vol. 54, no. 5, Oct. 2007, pp. 2583-2592.

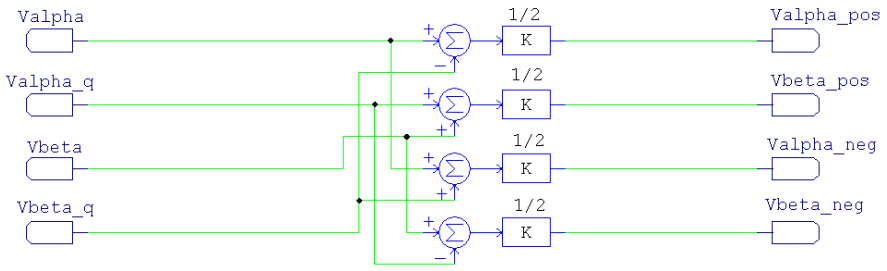

Figure 5-9. Line voltage symmetrical components extraction with SOGI quadrature signals

D. Line Synchronization

Once the current references are generated, they must be synchronized to the line voltages. At the highest level, line synchronization methods can be classified as either open loop or closed loop.[19] Open-loop methods generate the reference current vector directly from a line voltage vector without attempting to track any particular phase angle. Thus, they are suitable for implementation in the stationary reference frame. An example of an open-loop method based on low-pass filtered line voltages is shown in Figure 5-10. The line voltages *Vab*, *Vbc* and *Vca* are taken directly from the power circuit of Figure 4-1, low-pass filtered to attenuate harmonics, then transformed from the natural reference frame to the $\alpha\beta$ reference frame with a 30° phase shift such that *Valpha* is cophasor with *Van*. The $\alpha\beta$ voltage vector in Figure 5-10 (and the filter compensation *ph_shift* signal if the control method utilizes a negative sequence voltage vector) is then passed to the controller to achieve line synchronization in the stationary reference frame.

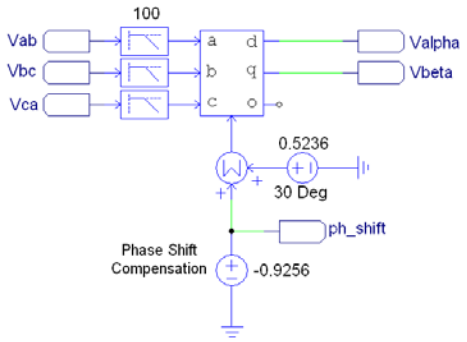

Figure 5-10. Open loop line synchronization model

Closed-loop methods (e.g., PLL) track a phase angle and align the reference current vector with this phase angle. In addition, the availability of phase angle information lends this method to implementation in the synchronously rotating dq reference frame or dual $dq^p$and dq^nreference frames.[20] A PLL-based synchronization scheme that tracks the angle of the positive sequence voltage vector (extracted from the line voltages via Figure 5-8 and Figure 5-9) is shown in Figure 5-11. It provides the *freq_est* signal needed to generate the quadrature voltage signals (Figure 5-8) as well as the *Vmag2_pos* signal (i.e., $\|\bar{v}^p\|^2$) to satisfy Eq. (5-10).

[19] M. Karimi-Ghartemani and M.R. Iravani, "A method for synchronization of power electronic converters in polluted and variable-frequency environments," *IEEE Transactions on Power Systems*, vol. 19, no. 3, pp. 1263-1270, Aug. 2004.

[20] Hong-Seok Song and Kwanghee Nam, "Dual current control scheme for PWM converter under unbalanced input voltage conditions," *IEEE Transactions on Industrial Electronics,* vol. 46, no. 5, pp. 953-959, Oct 1999.

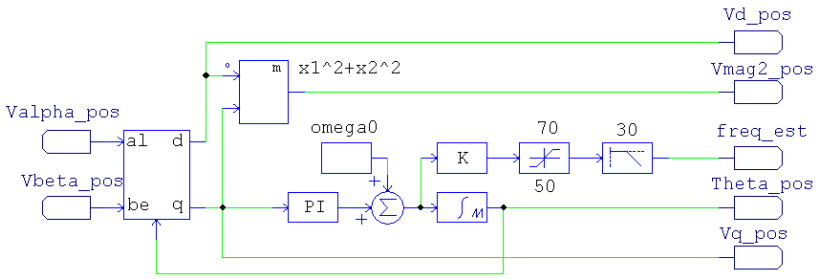

Figure 5-11. Positive sequence PLL model

A similar scheme that tracks the angle of the negative-sequence voltage vector can be constructed as shown in Figure 5-12. The negative-sequence voltage vector is the same frequency as the positive-sequence vector but opposite in rotation, so it is necessary to rotate this vector by twice the *ph_shift* compensation signal. As with the positive sequence PLL, the negative sequence PLL provides the Vmag2_neg signal (i.e., $\|\bar{v}^n\|^2$) necessary to satisfy Eq. (5-8).

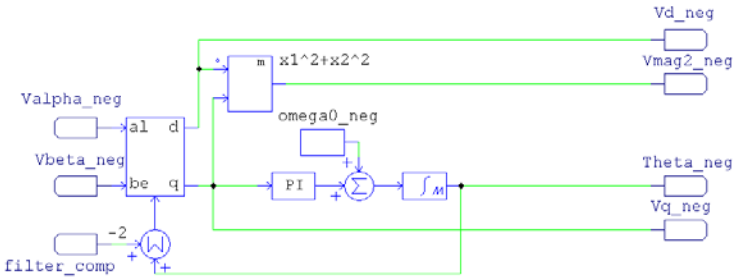

Figure 5-12. Negative sequence PLL model

The same control strategies discussed above (IARC, BPSC, PNSC) can then be implemented in the synchronous dq reference frame(s) using the [*Vd_pos, Vq_pos*] voltage vector, and, if applicable, the [*Vd_neg, Vq_neg*] voltage vector.

6. Symmetrical Fault Response

A. Introduction and Background

In Section 5, a control strategy was described, implemented as a *PSIM*® model, and simulated under asymmetrical grid fault conditions to determine the impact of the control method on the electromagnetic torque oscillations seen by the generator during these grid faults. In that document, it was shown that a control method known as PNSC can eliminate converter DC bus voltage oscillations, and therefore generator torque oscillations, during these transients.

In this section, the generator torque transients that occur for a variety of symmetrical (i.e., balanced three-phase) grid faults are characterized. The time-series electromagnetic torque outputs can then be utilized as a source of excitation for the dynamic model of the gearbox.

B. Power System and Control Model

The *PSIM*® implementation of the power system model utilized in these simulations is shown in Figure 4-1. The duration and severity (i.e., depth of voltage dip) of the faults are controlled through the timing of the switches and adjustment of the RL-branch impedances shown under the "Symmetrical Fault Generator" label. As in the previous section, the model represents one "quadrant" of the generator to be utilized in the dynamometer tests. All four quadrants operate in parallel with the same stator current, so the results of the single quadrant simulations can be scaled by a factor of four to represent a 1.5-MW drivetrain.

The control system is based on the PNSC method described in the previous section, with closed-loop (i.e., PLL) line synchronization. The *PSIM*® implementation of the control system is shown in Figure 5-8, Figure 5-9, Figure 5-11, and Figure 5-12. Unlike the asymmetrical fault cases considered earlier, symmetrical faults do not give rise to negative-sequence voltage, so the negative-sequence portion of the reference current generator simply remains inactive during balanced three-phase faults. That is, the PNSC method reverts to the BPSC method for balanced line voltages.

C. Simulations

Symmetrical short-circuit simulations were performed for grid faults corresponding to those used in the IEC 61400-21 testing protocol[21] and the FERC Order 661-A requirements for wind turbine generator fault ride-through.[22] In addition, a symmetrical fault at the high side of the local step-up (e.g., padmount) transformer was simulated. Initial conditions for each simulation were with the generator operating at its designed rated speed (190 rpm), rated power (375 kW per quadrant) and unity power factor. Simulated disturbances are summarized in Table 6-1.

---

[21] IEC 61400-21, *Edition 2: Wind Turbines - Part 21: Measurement and Assessment of Power Quality Characteristics of Grid Connected Wind Turbines*

[22] Federal Energy Regulatory Commission Order 661-A, Interconnection for Wind Energy, December 12, 2005, http://www.ferc.gov/EventCalendar/Files/20051212171744-RM05-4-001.pdf

Table 6-1. Symmetrical Fault Simulation Descriptions

Figure	Disturbance	Reference
Figure 6-1	30-cycle fault to 90% terminal voltage	IEC 61400-12, Table 1, Case VD1
Figure 6-2	30-cycle fault to 50% terminal voltage	IEC 61400-12, Table 1, Case VD2
Figure 6-3	12-cycle fault to 20% terminal voltage	IEC 61400-12, Table 1, Case VD3
Figure 6-4	9-cycle fault at high side of plant substation	FERC Order 661-A
Figure 6-5	9-cycle fault at high side of local transformer	Info only

Plots of converter line voltages, currents, active and reactive power, and generator electromagnetic torque for each of the simulations described in Table 6-1 are shown in Figures Figure 6-1 through Figure 6-5.

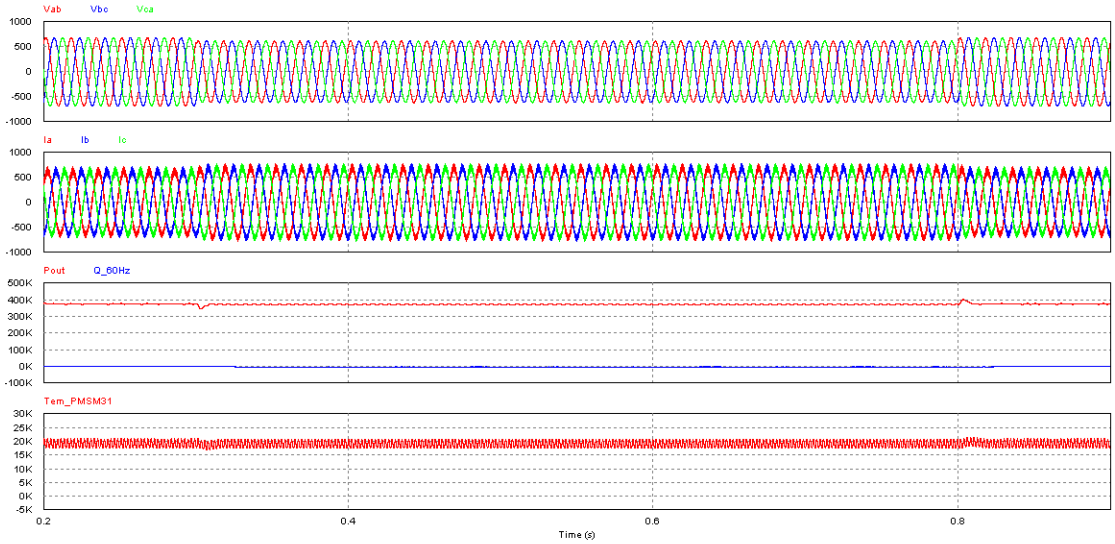

Figure 6-1. Thirty-cycle fault to 90% terminal voltage (Reference: IEC 61400-12, Table 1, Case VD1)

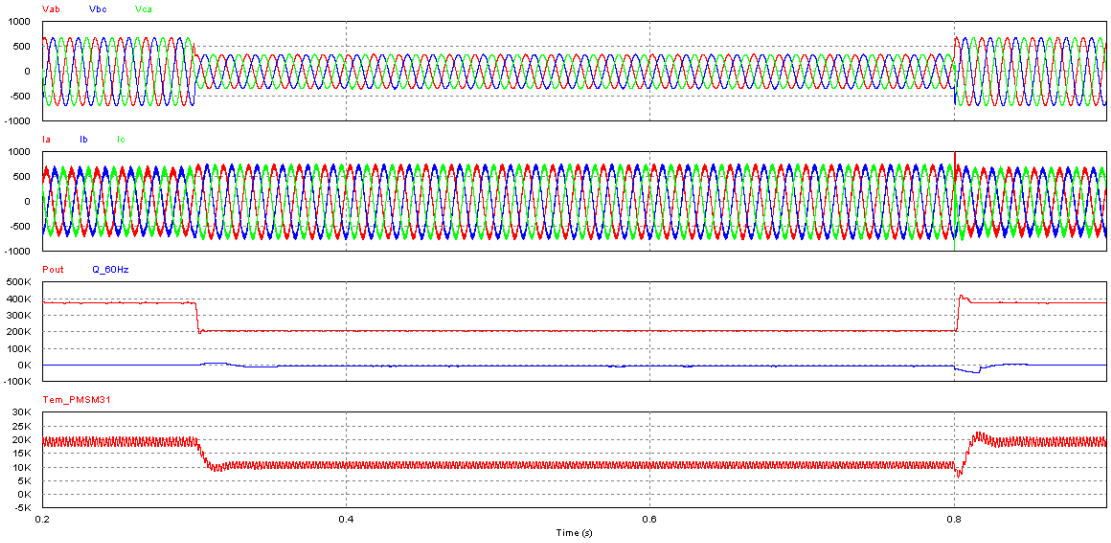

Figure 6-2. Thirty-cycle fault to 50% terminal voltage (Reference: IEC 61400-12, Table 1, Case VD2)

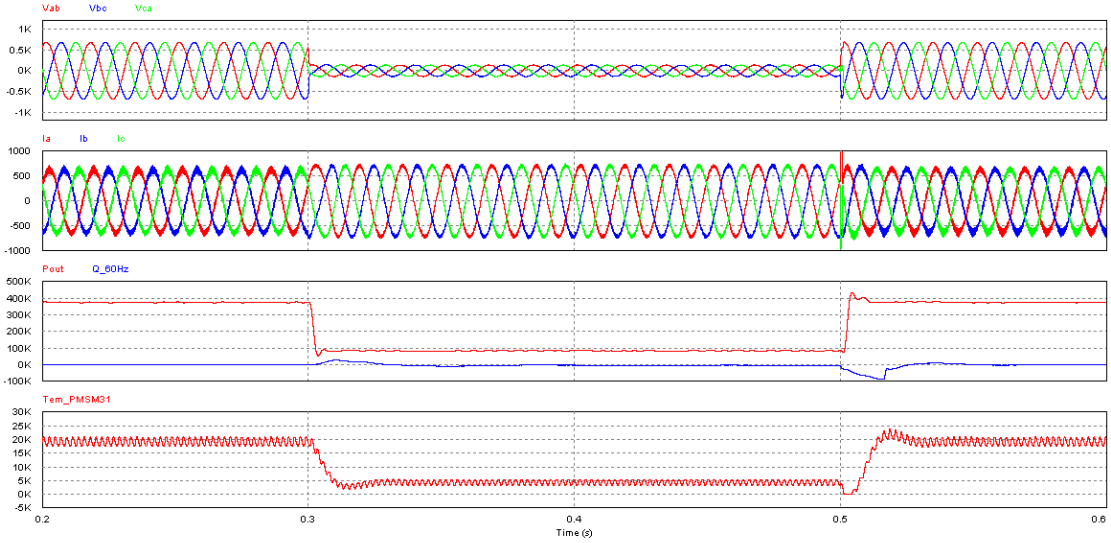

Figure 6-3. Twelve-cycle fault to 20% terminal voltage (Reference: IEC 61400-12, Table 1, Case VD3)

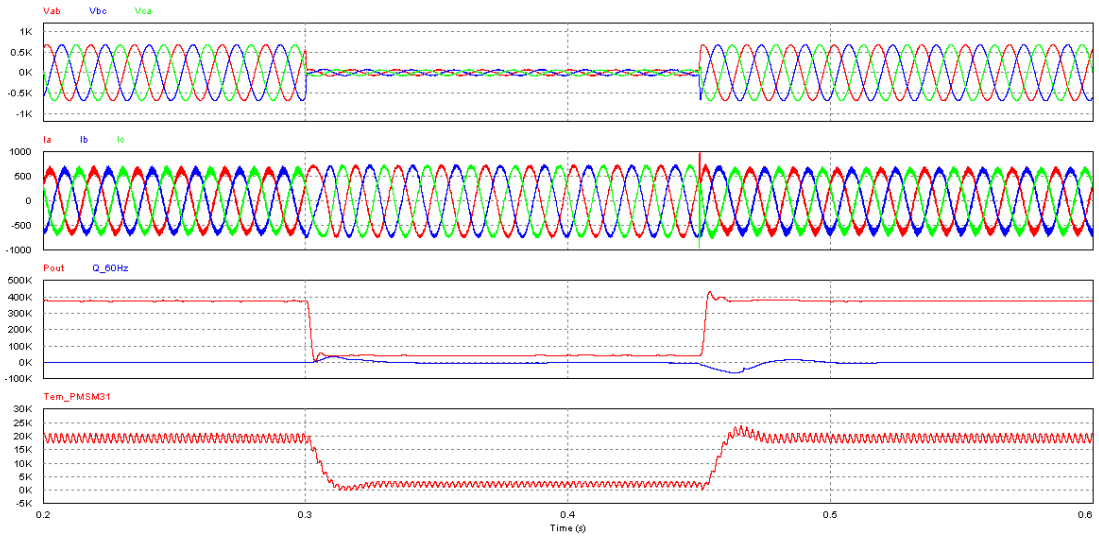

Figure 6-4. Nine-cycle fault at high side of plant substation (Reference: FERC Order 661-A)

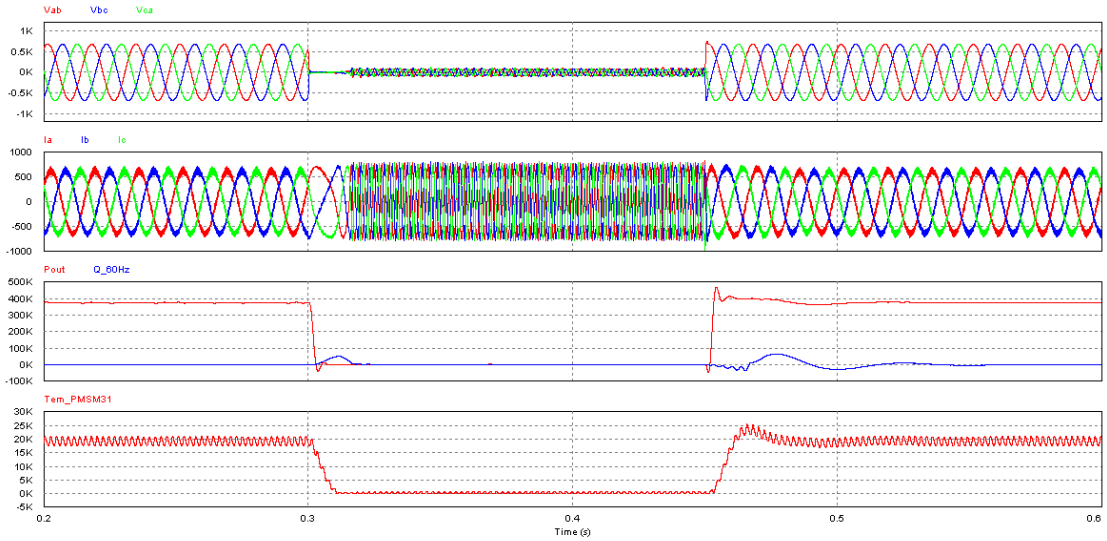

Figure 6-5. Nine-cycle fault at high side of local transformer, (Reference: Info, only)

D. Observations

1. For each fault, there are no positive-torque transients when the fault is applied. This is expected since the converter decouples the generator stator windings from the grid. The negative-torque transients at fault application in each case are a function of the converter current limit (*Ipmax_pk*) and corresponding output power limitations. There is little that can be done to economically mitigate this transient.

2. For the deep faults (Figure 6-2 through Figure 6-5), there are severe positive-torque transients upon fault clearing. This is a result of the converter being in current limit during the fault and the sudden increase in the line voltages that occurs at clearing. If this torque transient if of concern, the converter control system could be modified to drive the active component of its

output current to zero during the fault, then provide a controlled increase in active current (and, as a result, a controlled increase in active power and torque) in the post-clearing period.

3. For the fault location at the high side of the local step-up transformer (Figure 6-5), there is a sudden rise in the frequency of the converter output current during the fault. This is a result of the isolation of the converter from all external synchronous voltage sources. In a real wind turbine, this would result in the machine tripping on its overfrequency-protection function. It should be noted that no grid codes currently require ride-through capability for this fault location because clearing of the fault requires disconnection of the wind turbine from the grid.

7. Frequency Response

A. Introduction and Background

In this section, further modifications to the drivetrain model are proposed to provide an active power response to grid frequency transients. This response, referred to as primary-frequency response or governor control, is a feature of conventional turbo-generators that contributes to network stability following sudden changes to the load-generation balance. This feature was identified in Section 3 as an interconnection requirement in some of the target geographic markets.

Primary-frequency response is the method by which grid operators ensure that events that result in a sudden mismatch between load and generation are met by changes in generation that are proportional to the ratings of the individual generators on the network. These changes occur within the first few seconds following a sudden mismatch and are designed to arrest the change in system frequency until secondary measures (e.g., automatic generation control, or AGC) can be employed. These secondary measures then restore system frequency to its nominal value over a period of minutes. The proportional distribution of system generation changes are normally accomplished via so-called "droop" control, whereby the mechanical power of the prime mover is changed in proportion to the deviation of system frequency from its nominal value (60 Hz in the United States) once the deviation exceeds a specified deadband. The proportionality constant is referred to as the droop setting and is expressed as the ratio of the percentage frequency change to the desired power change in percent of the generator rating, as shown in Figure 7-1, Generator droop characteristic.

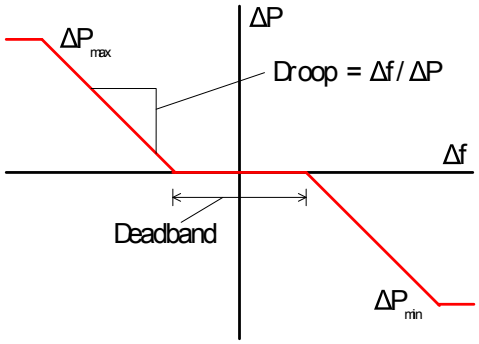

Figure 7-1. Generator droop characteristic

As an example, generators operating within the ERCOT footprint are required to operate with a deadband not exceeding ± 0.017 Hz and a 5% droop characteristic (i.e., a 5% increase/decrease in frequency beyond the deadband should drive a corresponding 100% decrease/increase in generator power). Wind generator underfrequency response is required only if the wind plant is operating in a curtailed condition with respect to the prevalent wind resource due to a previous overfrequency event or other ERCOT-initiated curtailment. Further, the underfrequency response requirement is limited to the curtailed power at the time of the event.

B. Power System and Control Model

The *PSIM*® implementation of the power system model of Figure 4-1 is utilized in these simulations. The control system is based on the PNSC method described in Section 5.B.3. As with the symmetrical fault simulations in the previous section, frequency deviation is a balanced three-phase phenomenon, so the negative sequence portion of the reference current generator simply remains inactive during these events.

A form of governor control to implement the droop characteristic of Figure 7-1 was added to the model. This is shown in Figure 7-2 below. The output of the governor is a multiplier (*P_mul*) applied to the commanded active power. The input is the estimated frequency signal generated from the positive sequence PLL of Figure 5-11 above. For purposes of the simulations performed in this section, the deadband was set to ±1.0 Hz, and the gains (*K*) were set to 0.33, which corresponds to a 5% droop; i.e., 1/(0.33*60) = 0.05. In large, interconnected networks, the actual deadband is much smaller. The values used here were selected so that the effect of the deadband is visible in the simulation results.

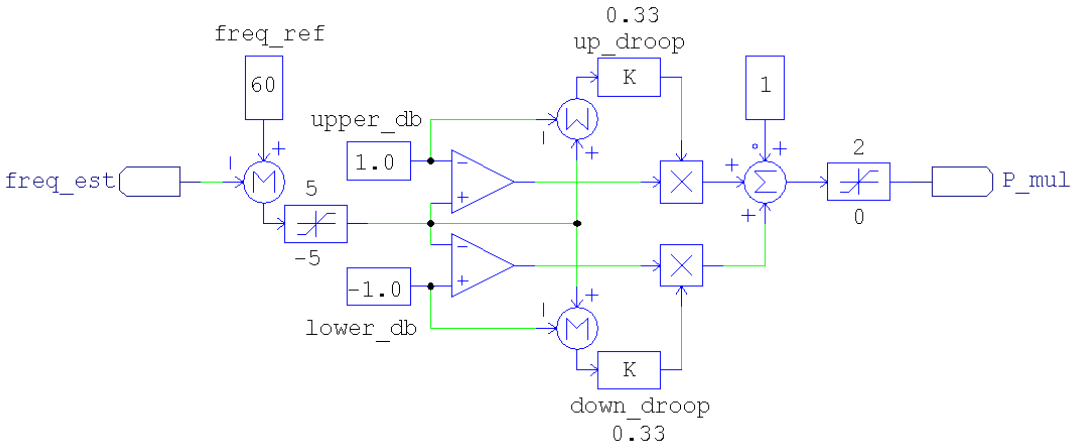

Figure 7-2. Governor control model

C. Simulations

Simulations of overfrequency and underfrequency transients were performed first with the generator operating at its designed rated speed (190 rpm) and power (375 kW per quadrant). Next, the same transients were simulated with the generator operating 50% of rated power (177.5 kW per quadrant) and at 150 rpm, the speed corresponding to 50% power assuming a cubic power-speed curve below rated output. Simulation initial conditions and disturbances are summarized in Table 7-1.

Table 7-1. Frequency-Response Simulation Descriptions

Figure	Initial Conditions			Disturbance
	Speed	Pref	Qref	
Figure 7-3	190 rpm	375 kW	0 kVAr	Overfrequency transient to 64 Hz
Figure 7-4	190 rpm	375 kW	0 kVAr	Underfrequency transient to 56 Hz
Figure 7-5	150 rpm	177.5 kW	0 kVAr	Overfrequency transient to 64 Hz
Figure 7-6	150 rpm	177.5 kW	0 kVAr	Underfrequency transient to 56 Hz

Plots of converter line voltages, actual and estimated line frequencies, line currents, active and reactive power, and generator electromagnetic torque for each of the simulations described in Table 7-1 are shown in Figure 7-3 through Figure 7-6.

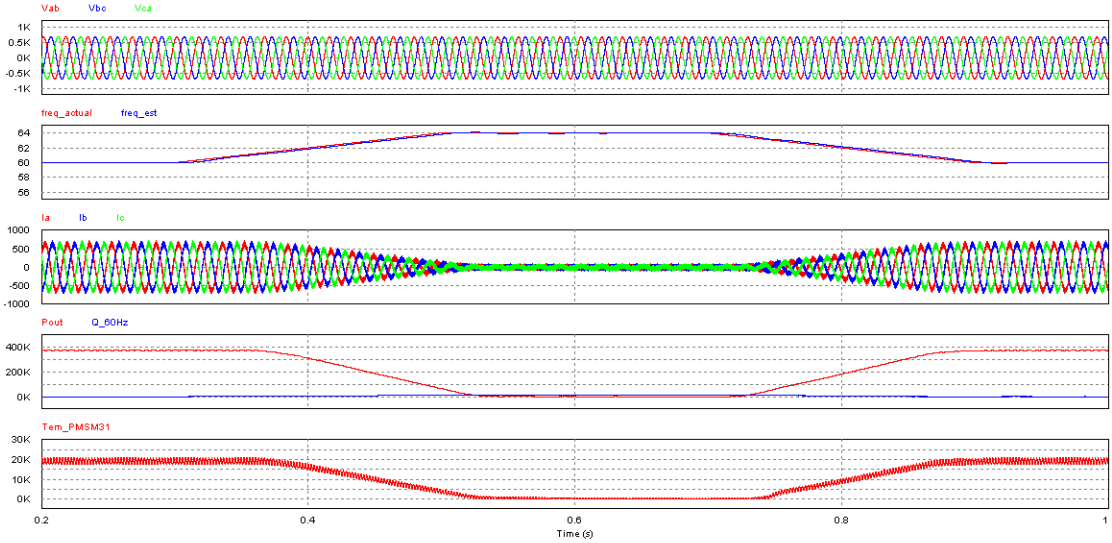

Figure 7-3. Overfrequency transient at rated power

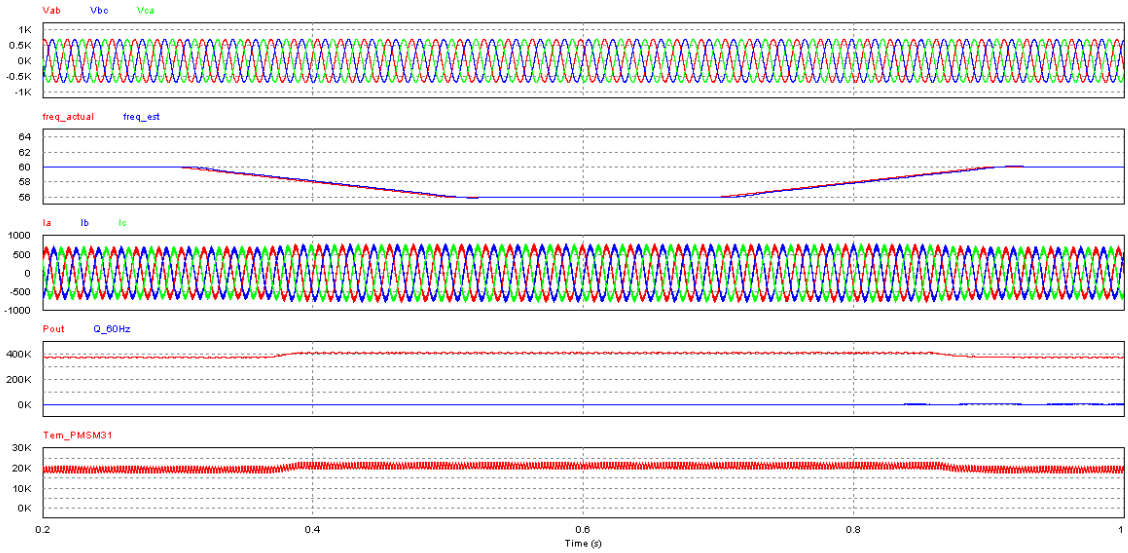

Figure 7-4. Underfrequency transient at rated power

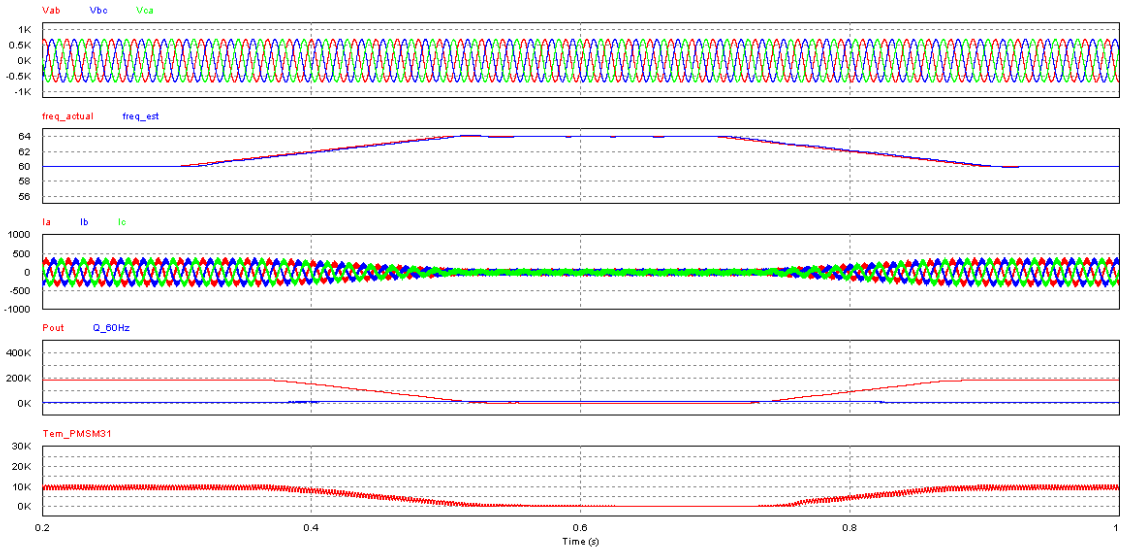

Figure 7-5. Overfrequency transient at 50% power

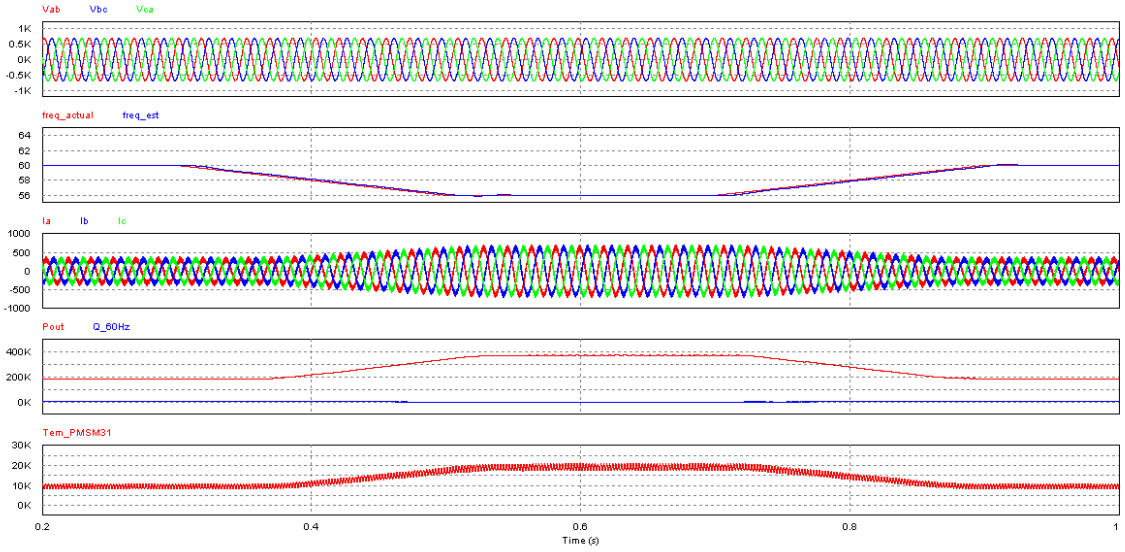

Figure 7-6. Underfrequency transient at 50% power

D. Observations

1. In each simulation, the frequency estimate closely tracks the actual frequency. Further, the ability to tightly control the power factor under steady-state frequency deviations as much as 7% from nominal is an indication of good PLL performance.

2. The active power output is responsive to the droop characteristic in all cases except for the underfrequency event at rated output power (Figure 7-4). The output power in this simulation is limited as a result of the converter current limit (*Ipmax_pk*).

3. For the underfrequency event at 50% power (Figure 7-6), generator torque is quite high (nearly 130% of rated torque). In a real wind turbine, this would not occur as the turbine controller

would allow the rotor speed to rise such that torque would not exceed rated. So this result is an artifact of the model (turbine speed control is not included) and not a technical concern.

8. Main-Shaft Damping

A. Introduction and Background

In this section, the torsional mode associated with the compliant main shaft is addressed. The drivetrain has natural torsional modes that can be excited by a variety a stimuli (changes in wind speed, control actions, etc.), so damping of this mode is not an explicit grid interconnection requirement, per se. However, particularly intense sources of excitation for these resonances are grid faults that are electrically near the wind plant. Excitation of these torsional modes in the drivetrain can result in damaging speed and torque oscillations.

The main-shaft torsional mode is normally characterized using the two-mass representation shown in Figure 8-1.[23, 24] The wind turbine rotor and generator inertias are J_{rot} and J_{gen}, respectively. The aerodynamic torque applied to the rotor is T_{rot}, while the opposing generator electromagnetic torque is T_{em}. The rotor and generator speed and angle are θ and ωin the directions defined in the figure. The spring labeled K_s is the main-shaft stiffness, while the dashpot labeled D_s represents viscous damping. The gearbox is not shown in this model, thus it is assumed that all mechanical parameters have been reflected to either the high-speed or the low-speed shafts, taking the gearbox ratio into proper account. The self-damping terms for the wind turbine rotor (aerodynamic resistance) and generator (frication and windage) are ignored.

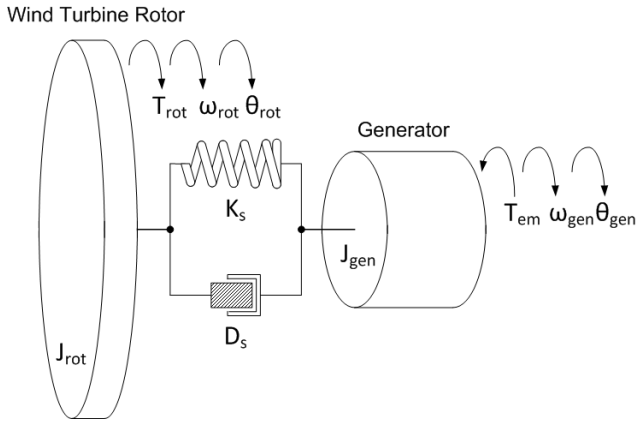

Figure 8-1. Two-mass representation of torsional dynamics

With respect to the main-shaft twist, the system has a single degree of freedom, the angle ($\theta_{rot} - \theta_{gen}$). The dynamics equations for the two-mass model are as follows:

$$T_{rot} = J_{rot}\ddot{\theta}_{rot} + K_s(\theta_{rot} - \theta_{gen}) + D_s(\dot{\theta}_{rot} - \dot{\theta}_{gen}) \quad (8\text{-}1)$$

[23] P. Sørensen, A. Hansen, L. Janosi, J. Bech, and B. Bak-Jensen, *Simulation of Interaction between Wind Farm and Power System,* Risø-R-1281(EN), Risø National Laboratory, Roskilde, December 2001.
[24] A. Rolán, A. Luna, J. Rocabert, D. Aguilar, and G. Vazquez, "An Approach to the Performance-Oriented Model of Variable-Speed Wind Turbines," *2010 IEEE International Symposium on Industrial Electronics (ISIE)*, 4-7 July 2010.

$$T_{em} = J_{gen}\ddot{\theta}_{gen} + K_s(\theta_{gen} - \theta_{rot}) + D_s(\dot{\theta}_{gen} - \dot{\theta}_{rot}) \quad (8\text{-}2)$$

Subtracting (8-2) from (8-1), some additional algebraic manipulation yields:

$$\frac{T_{rot}J_{gen} - T_{em}J_{rot}}{J_{rot}+J_{gen}} = \frac{J_{rot}J_{gen}}{J_{rot}+J_{gen}}(\ddot{\theta}_{rot} - \ddot{\theta}_{gen}) + D_s(\dot{\theta}_{rot} - \dot{\theta}_{gen}) + K_s(\theta_{rot} - \theta_{gen}) \quad (8\text{-}3)$$

(8-3) is a second-order differential equation whose unforced response is of the form $\ddot{x} + 2\zeta\omega_0\dot{x} + {\omega_0}^2 x = 0$, where ω_0 is the natural frequency and ζ is the damping ratio. So the natural frequency and damping ratio for the system in Figure 8-1 are:

$$\omega_0 = \sqrt{\frac{K_s}{\frac{J_{rot}J_{gen}}{J_{rot}+J_{gen}}}} \quad (8\text{-}4)$$

$$\zeta = \frac{D_s}{2K_s} \cdot \omega_0 \quad (8\text{-}5)$$

In a wind turbine application, where $J_{rot} \gg J_{gen}$, (8-4) can be approximated with high accuracy as:

$$\omega_0 \cong \sqrt{\frac{K_s}{J_{gen}}} \quad (8\text{-}6)$$

For the NGD, analysis by others provided known values of generator inertia (J_{gen}) and the main-shaft stiffness (K_s). The viscous damping coefficient (D_s) was determined by matching the response of the drivetrain model to transient test data collected earlier. These mechanical parameters are summarized in Table 8-1.

Table 8-1. Torsional Model Parameters (Referred to High-Speed Shaft)

Parameter	Value
J_{gen}, Generator Moment of Inertia	1,350 kg-m^2
$\boldsymbol{K_s}$, Main-Shaft Stiffness	4.0 x 10^6 N-m/rad
$\boldsymbol{D_s}$, Viscous Damping Coefficient	2,000 N-m-s/rad

These torsional model parameters, when applied to (8-6) and (8-5), result in a natural frequency of 54.5 rad/s (or 8.6 Hz) and a damping ratio of 0.014.

For modeling purposes, the drivetrain equations can be translated from a mechanical system to an electric system by using an RLC circuit with the same natural frequency and damping ratio. In the electrical analogy, voltages represent speed and currents represent torque. The unforced response of a parallel RLC circuit is:

$$C\,\ddot{v} + \frac{1}{R}\dot{v} + \frac{1}{L}v = 0 \quad (8\text{-}7)$$

Comparing (8-7) and (8-2), it can be seen that C is analogous to J_{gen}, $\frac{1}{L}$ is analogous to $\boldsymbol{K_s}$, and $\frac{1}{R}$ is analogous to D_s. Figure 8-2 shows the main-shaft model utilized in the simulations in this section. The voltage at the node to the immediate right of the mechanical/electrical interface block (labeled

M/E in Figure 8-2) is the generator shaft speed, and the current injected into the right side of this block is the mechanical torque applied to the generator shaft.

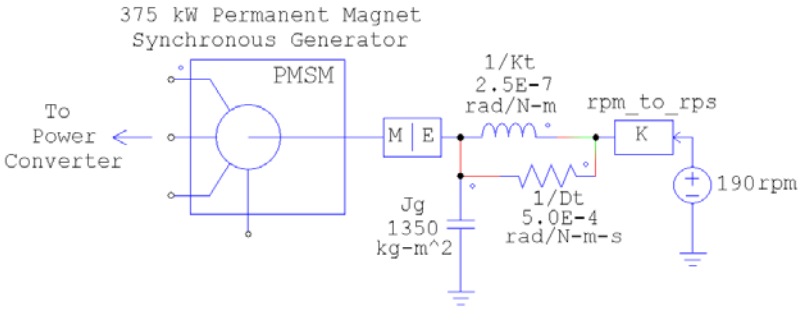

Figure 8-2. Main-shaft torsional model

B. Power System and Control Model

The *PSIM*® implementation of the power-system model utilized in these simulations is that of Figure 4-1, but with the single-mass, constant-speed mechanical model replaced with the two-mass torsional model of Figure 8-2. The control system is based on the PNSC method described in Section 5.B.3.

An additional algorithm to provide active damping of the main-shaft torsional mode by the power converter has been included and is shown in Figure 8-3. Torsional oscillations in the generator result in oscillations of the converter DC link voltage, so it is possible to provide active damping of this mode without a speed sensor. The DC link voltage is monitored and processed through a bandpass filter with transfer function:

$$H(s) = \frac{kBs}{s^2+Bs+\omega_c^2} \qquad (8\text{-}8)$$

where k is the gain, B is the width of the passing band and ω_c is the center frequency of the filter. The filter is tuned to the torsional resonant frequency and provides an output signal that is used to modify the active power command (P_{ref}) in Figure 5-5. This auxiliary power command is limited to ±10% (±375 kW) of the nominal rating of the power converter.

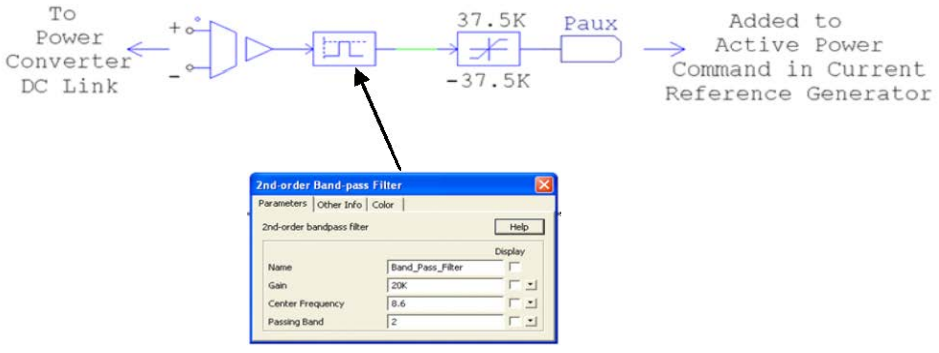

Figure 8-3. Active main-shaft damping control model

C. Simulations

Simulations were performed to demonstrate the effect of the active damping algorithm described in Section 8.B above for both changes in the active power command (P_{ref}) and for grid fault at the high side of the wind plant substation. Initial conditions for each simulation were with the generator operating at its designed rated speed (190 rpm) and power (375 kW per quadrant). A description of each simulation is included in Table 8-2.

Table 8-2. Main-Shaft Torsional Mode Simulations

Figure	Disturbance
Figure 8-4	Two step changes in commanded power of -125 kW each; active damping disabled
Figure 8-5	Two step changes in commanded power of -125 kW each; active damping enabled
Figure 8-6	Nine-cycle, three-phase fault at high side of wind plant substation; active damping disabled
Figure 8-7	Nine-cycle, three-phase fault at high side of wind plant substation; active damping enabled

Plots of converter active power, generator electromagnetic torque, high-speed shaft torque, high-speed shaft speed, and DC link voltage for each of the simulations described in Table 8-2 are shown in Figure 8-4 through Figure 8-7.

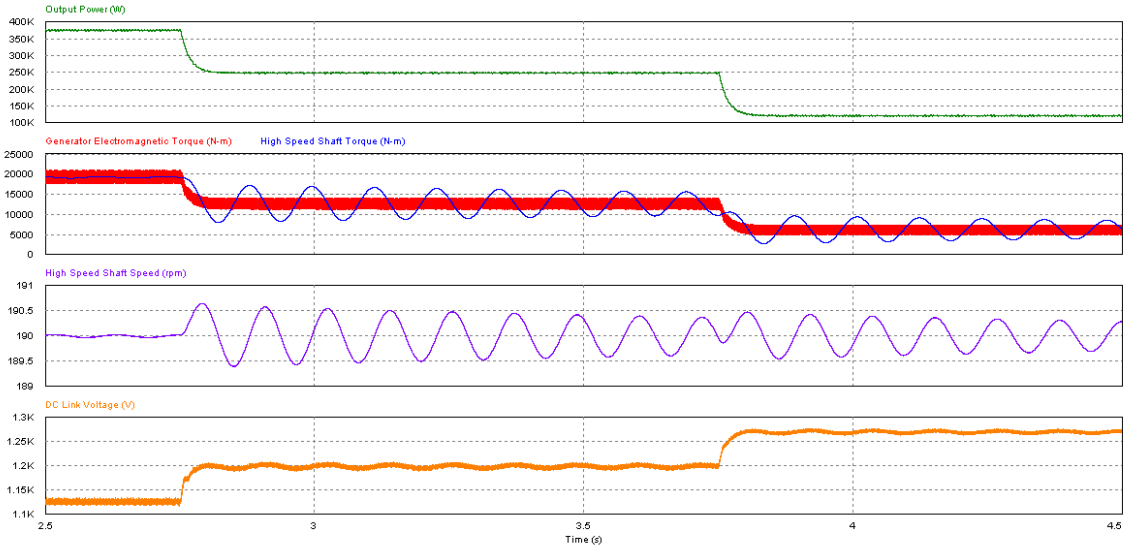

Figure 8-4. Power command step changes—no active damping

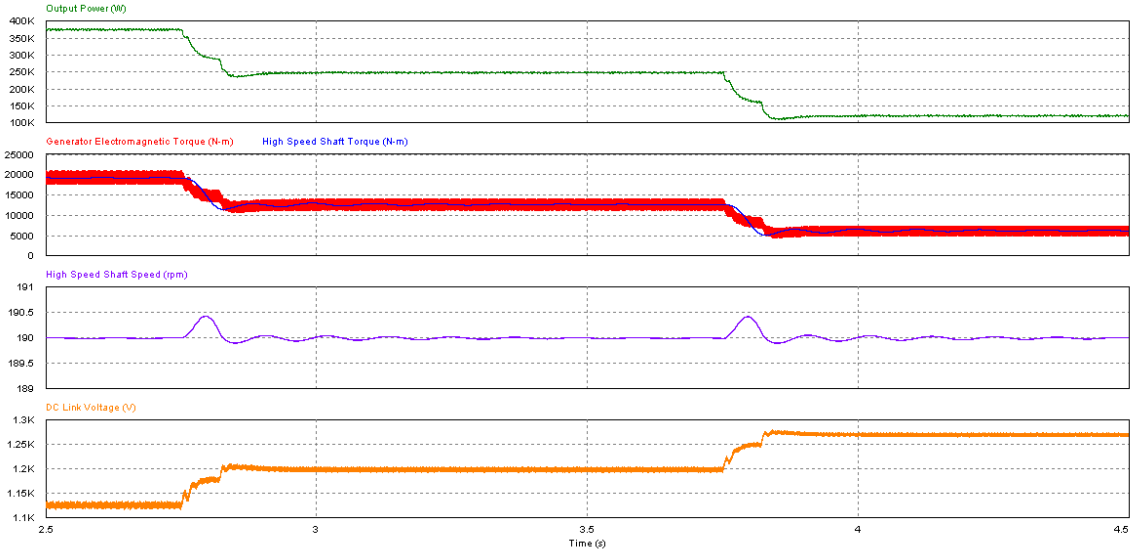

Figure 8-5. Power command step changes—with active damping

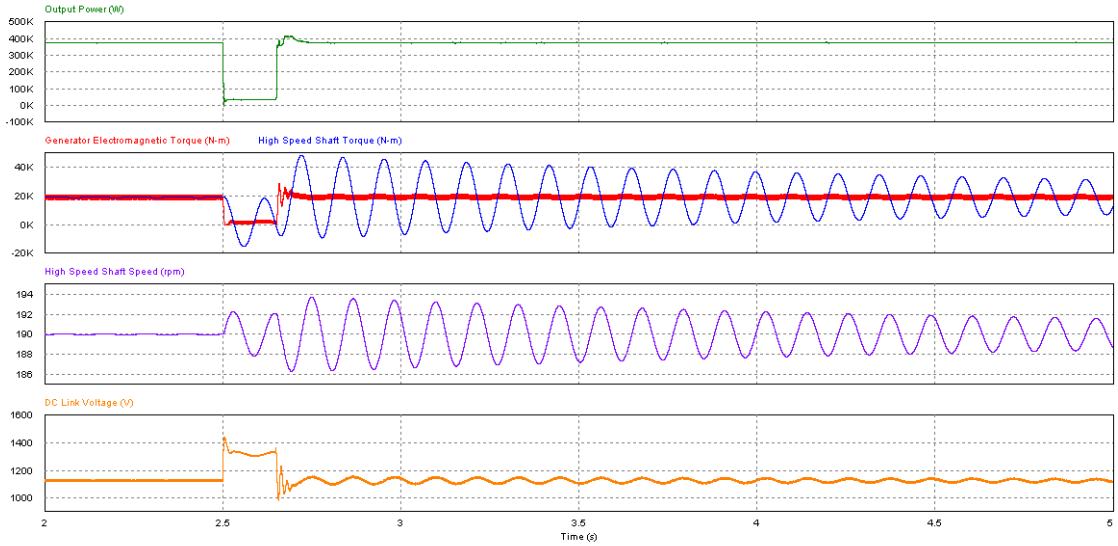

Figure 8-6. Nine-cycle symmetrical fault at high side of substation—no active damping

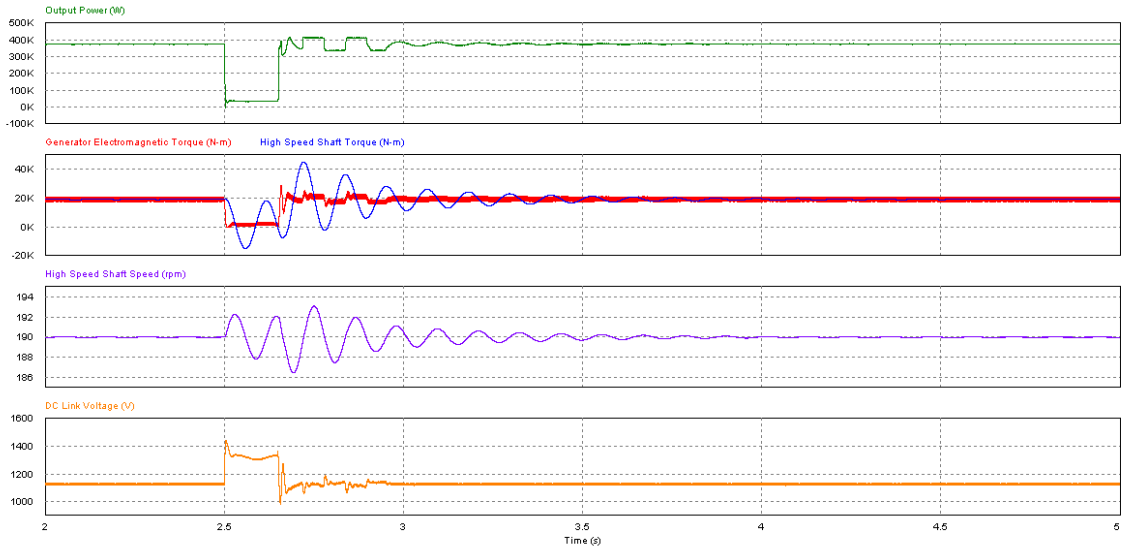

Figure 8-7. Nine-cycle symmetrical fault at high side of substation—with active damping

D. Observations

1. The active damping algorithm proposed is effective at damping the main-shaft mode within one resonant frequency cycle for step changes in power as much as 33% of rating.

2. Main-shaft mode damping for the case of a symmetrical fault at the high side of the substation is effective, but requires five to six resonant frequency cycles to completely damp these torque and speed oscillations. The reason for this is the severity of the excitation (nearly ±100% changes in active power) due to the fault as well as the ±10% limitation imposed on damping power. These oscillations could be damped more quickly if the converter had short-term (1–2 seconds) overload capability that could be utilized to provide damping power.

9. Conclusions

A list of interconnection issues to be addressed in the design of the power converter control software for the NREL NGD was developed by reviewing the grid interconnection requirements of various North American transmission system operators. A subset of those requirements that presented the greatest impact to the wind turbine drivetrain design was then selected for mitigation via power converter control algorithms. This subset included:

1. Ride-through capability for symmetrical and asymmetrical grid faults
2. Governor response for grid frequency deviation
3. Main-shaft torsional mode damping.

It was determined that the current control method known as PNSC can provide high-quality current waveforms and allows for cancellation of the second harmonic component of active power during asymmetrical faults by generating asymmetrical output currents. For symmetrical faults, the PNSC method automatically reverts to a second control method known as BPSC. The BPSC method generates symmetrical currents in response to both balanced and unbalanced line voltages, so this method is suitable for applications where the DC link capacitance is sufficient to limit the generator torque oscillations during asymmetrical faults to an acceptable level.

An algorithm that allows the drivetrain to participate in Primary Frequency Response (modulation of output power in response to grid-frequency deviations) was developed and simulated. Due to the slow rate at which the grid frequency changes during generation-load mismatch conditions, this feature is not anticipated to impose design criteria for the drivetrain beyond those driven by normally occurring wind turbulence.

Finally, it was shown that grid faults are major sources of excitation for natural torsional resonances in the drivetrain that can result in damaging speed and torque oscillations. An algorithm that uses power converter DC link voltage sensing to provide active damping of the most significant of these torsional modes was developed and demonstrated through computer simulation.